Master Thesis

Superconductor-Insulator Quantum Phase Transitions in a Dissipative Environment

Rasmus Renberg

Department of Physics,
School of Engineering Sciences
Royal Institute of Technology, SE-106 91 Stockholm, Sweden

Stockholm, Sweden 2018

Typeset in LaTeX

Scientific thesis for the degree of Master of Engineering in the subject area of Theoretical physics.

TRITA-SCI-GRU 2018:407

Printed in Sweden by Universitetsservice US AB, Stockholm November 2018

8@ §}9H§

Monte Carlo simulations are used to study superconductor-insulator quantum phase transitions in Josephson junction chains coupled to a dissipative environment. Starting from the quantum phase model to describe the Josephson junction chain, and representing the dissipative environment as semi-infinite transmission lines, we end up with a formulation that is suitable to study chains of varying length. An inverse effective capacitance is defined and used to determine whether the system is in a superconducting or an insulating state. The Schmid(-Bulgadaev) transition for a single junction, and the transition first predicted by Bradley and Doniach for an infinite chain, are both studied. We also examine the dependence of the phase transitions on the charge screening length . Although the results of the simulations seem to at least in part agree with theory, some discrepancies with other studies are found. These discrepancies need further study to be explained.

b0´ °n}L : Josephson junction, Josephson junction chain, one-dimensional Josephson junction array, superconductor-insulator quantum phase transition.

~9h h9jT9§§j_jX

Monte Carlo-simuleringar används för att studera kvantfasövergångar mellan supraledande och isolerande faser i kedjor av Josephsonövergångar kopplade till en dissipativ omgivning. Med den så kallade kvantfasmodellen som utgångspunkt för att beskriva Josephsonkedjan, och genom att representera den dissipativa omgivningen som halvoändliga transmissionslinjer, kommer vi fram till en formulering som lämpar sig för att studera kedjor av varierande längd. En effektiv invers kapacitans definieras och används till att avgöra huruvida systemet är i en supraledande eller en isolerande fas. Både Schmid(-Bulgadaev)-fasövergången för en enda Josephsonkoppling, och fasövergången som först predikterades av Bradley och Doniach för en oändlig kedja, studeras. Vi undersöker även fasövergångarnas beroende på laddningsavskärmningslängden . Även om resultaten av simuleringarna åtminstone delvis verkar överensstämma med teorin, upptäcks några diskrepanser mellan dessa och resultaten från andra studier. Dessa diskrepanser behöver analyseras vidare för att förklaras.

i ´HcOen}LI Josephsonövergång, Josephsonövergångskedja, supraledare-isolator kvantfasövergång.

8 Hc j n ° eOLX h O j §

This master thesis was carried out from February to November 2018, at the Department of Theoretical Physics at the Royal Institute of Technology (KTH). I would especially like to thank my supervisor Jack Lidmar for introducing me to this area of physics and for his invaluable expertise and input. I want to thank my friends and fellow thesis workers Pontus von Rosen and Martin Lindberg for all the help and laughs they have given me in the last year. Lastly, I want to thank my family for their unconditional support.

Gnj§0j§

G \9q§0} o

^j§}nL«H§_nj

Although superconductivity was first discovered more than 100 years ago by Holst and Onnes in 1911 [1], it is still a highly active field in physics. High-temperature superconductors, the application of superconductors in quantum computers and superconductivity in one and two dimensions are only a few subjects in this area with ongoing research.

The longevity of superconductivity as a research topic can be attributed to the simple fact that it is a difficult problem to deal with. It took more than 40 years after its discovery until a satisfactory microscopic theory, called the BCS theory, of (low-temperature) superconductors was found.

Before this, superconductivity was best understood using phenomenological models. One of the most successful of these, which could explain phenomena that were beyond the scope of other existing theories, was introduced in 1950 by the Soviet physicists Vitaly Ginzburg and Lev Landau [1, 2]. Despite the accomplishments of the Ginzburg-Landau (GL) theory, its importance was, due to its phenomenological nature, not generally appreciated, especially in western literature [2]. This changed in 1959 when Gor'kov was able to derive the GL theory as a rigorous limiting case of the BCS theory.

In 1962, shortly after the publication of the BCS theory, Brian Josephson, then a graduate student, published a stunning article in which he considered the tunneling of electrons between two superconductors which were separated by a thin insulating barrier [1, 2]. Using BCS theory, he found the remarkable result that a current can flow between the superconductors, even when there is no potential difference between the two. His theory also predicted that the application of a constant potential leads to an alternating current. A system consisting of two superconductors separated by a thin insulating layer is now called a Josephson junction.

Today Josephson junctions have widespread applications (see e.g. [3]): they are used to construct so called SQUIDs, which are magnetometers used to measure very small changes in magnetic fields; they are used world-wide in industry and laboratories to *L0»j0* the standard volt; they can be used to construct photon and

particle detectors; and they can be used in microwave photonics. In the last two decades, quantum bits based on Josephson junctions have shown great promise as the building block of practical quantum computers.

Even disregarding their applications, Josephson junctions in themselves display a wide range of interesting phenomena. For example, Josephson junction arrays, i.e. regular networks of superconducting islands weakly coupled by tunnel junctions, are ideal model systems to study classical phase transitions and vortex dynamics [4]. Another highly interesting phenomenon in Josephson arrays is quantum phase transitions, i.e., phase transitions at zero temperature due to quantum fluctuations. The parameter controlling the transition in Josephson arrays is the ratio E_J/E_C where E_J is the Josephson coupling energy and E_C corresponds to the energy needed to add an extra electron charge to a neutral island. The quantum phase transition means that by varying the ratio E_J/E_C, one can turn the Josephson junction array from a superconducting state into an insulating state even though each island is superconducting. The critical value of E_J/E_C for an infinite one-dimensional Josephson array, i.e., a Josephson chain, was first calculated by Bradley and Doniach [5]. These results were later extended by Korshunov [6] and Choi et al.[7]

An effect that is always present in macroscopic system, such as a Josephson junction, is that of dissipation, i.e. the energy transfer from the system to the environment. This was pointed out by Caldeira and Leggett in 1982 [8], who introduced a general model to describe the effect of dissipation on quantum tunneling. Shortly thereafter, Schmid and Bulgadaev [9, 10] applied this theory to a Josephson junction and found that varying the strength of dissipation to the environment can make the junction transition from a superconducting state to an insulating state. This quantum phase transition is now called the Schmid(-Bulgadaev) transition.

In this thesis we aim to use Monte Carlo simulations to study the phase transitions in Josephson junction chains coupled to a dissipative environment. This environment is taken to be two semi-infinite transmission lines, each coupled to either side of the chain. In contrast to what is commonly done when studying chains of Josephson junctions, non-periodic boundary conditions will be used. The average current flowing in the system is fixed to zero, and charge conservation is enforced, i.e. the system is modeled as a canonical ensemble. However, the voltage drop across the chain is allowed to fluctuate. This allows us to compute an effective inverse capacitance of the chain which can be used to determine whether the system is in a superconducting or an insulating state. The length of the chain can be varied, and, in our simulations, it ranges from consisting of 1 up to 39 junctions. We will also consider the effect of the so-called charge screening length on the phase transitions.

The thesis is structured as follows: chapter 2 will give a brief introduction to the physics of Josephson junctions and chains, including calculations necessary for the simulations. Chapter 3 will describe the Monte Carlo simulations employed in this thesis. The results of the simulations are displayed in chapter 4 and a discussion of them together with a conclusion is given in chapter 5.

G\9q§O} ©

`n Oq\ nj a«jH§_nj 9jL H\9_j

This chapter covers a brief overview of single Josephson junctions and a more thorough investigation of chains of Josephson junctions. As a starting point, section 2.1 is dedicated to give a minimal introduction to the Ginzburg-Landau (GL) theory of superconductivity. Much more comprehensive accounts can be found in e.g. [2, 11, 12]. In section 2.2 we will then use this theory to try to understand the equations that govern Josephson junctions. We will then make a slight necessary detour in section 2.3 where we briefly describe the results of Schmid and Bulgadaev. In sections 2.4 - 2.6 we go on describing the physics of a Josephson chain coupled to transmission lines on either sides, and how the 1-dimensional quantum system can be mapped onto a (1 + 1)-dimensional classical system. In section 2.7 we describe the system in an alternative way and see that this makes it possible to define an effective inverse capacitance which is a suitable quantity to compute in the simulations.

©uo 8 h_j_h9e _j§}nL«H§_nj §n §\O W_j¶@«}X]d9jL9« hnLOe

The Ginzburg-Landau model of superconductivity was inspired by Landau's previous work on second order phase transitions [11]. Motivated by this, they postulated that the transition from the normal state to the superconducting state could be described by a complex order parameter , also called the macroscopic wavefunction. This was assumed to be 0 in the metallic state and non-zero in the superconducting state, i.e. it obeyed

$$= \begin{cases} 0; & T > T_c \\ j\ j e^{i} ; & T < T_c \end{cases} ; \tag{2.1}$$

where T_c is the critical temperature and ϕ is the q\9 0 of the macroscopic wave-function. When the model was conceived, it was not clear what physical quantity was representing. However, thanks to Gor'kov, we now know that is, disregarding some numerical constants, equal to the superconducting gap [11]. $j\ j^2$ can in in fact be identified as the density of Cooper pairs.

GL went on and postulated that the free energy in the superconducting state F_s was given by [2, 11]:

$$F_s = F_n + \int a(T)j\ j^2 + \frac{b(T)}{2}j\ j^4 + \frac{1}{2m}\left|\frac{\sim}{i}r\quad qA\right|^2 + \frac{(r\quad A)^2}{2\ _0}\ d^3r; \quad (2.2)$$

where F_n is the free energy in the normal state, $a(T)$ and $b(T)$ are some phenomenological parameters, and $\mathbf{A}$ is the magnetic vector potential. Note that SI units are used. GL argued that $b(T) > 0$ for all values of T, and that $a < 0$ for $T < T_c$ and $a > 0$ for $T > T_c$. m and q are the mass parameter and charge, respectively, associated with . Usually these are set to the mass and charge of a Cooper pair, i.e. $m = 2m_e$, $q = 2e$ [12].

The order parameter is found by locating the minimum free energy of the system. This is most conveniently done by using the functional derivatives for the independent functions $(\mathbf{r})$, $(\mathbf{r})$ and $\mathbf{A}(\mathbf{r})$, leading to the equations

$$0 = \frac{F}{(\mathbf{r})}; \quad 0 = \frac{F}{(\mathbf{r})}; \quad 0 = \frac{F}{\mathbf{A}(\mathbf{r})}: \quad (2.3)$$

It turns out that $0 = \frac{F}{(\mathbf{r})}$ and $0 = \frac{F}{(\mathbf{r})}$ yields the same equation:

$$\frac{\sim^2}{2m}\ r + \frac{2ei}{\sim}\mathbf{A}\ ^2\ (\mathbf{r}) + (a + bj\ j^2)\ (\mathbf{r}) = 0: \quad (2.4)$$

$0 = \frac{F}{\mathbf{A}(\mathbf{r})}$ yields the following equation

$$\mathbf{j}_s = \frac{i\sim e}{m}(\quad r\qquad r\quad) \quad \frac{(2e)^2}{m}\mathbf{A}j\ j^2; \quad (2.5)$$

where we have used that $\mathbf{B} = r\quad \mathbf{A}$ and $r\quad \mathbf{B} = {}_0\mathbf{j}_s$ where $\mathbf{j}_s$ is the density of the supercurrent. Equations (2.4) and (2.5) are called the W_j¶@«}X]d9jL9« 0x«9§_nj . Let us first consider (2.4) with no magnetic field and a weak gradient in . The non-trivial solution, when $a(T) < 0$, is then given by

$$j\ j^2 = j\ _1 j^2 = \frac{a(T)}{b(T)}; \quad (2.6)$$

where the notation $_1$ is used since approaches this value infinitely deep in the superconductor [2]. Now, if we introduce variations in then (2.4) in 1-dimension can be written as:

$$\frac{\sim^2}{2m\ jaj}\frac{d^2f}{dx^2} + f\quad f^3 = 0; \quad (2.7)$$

where $f = = _1$. It is natural to define a characteristic length ^{2} $\frac{\sim^2}{2m\ jaj}$. is called the W_j¶@«}X]d9jL9« Hn\0}0jH0 e0jX§\. This characterizes a length for the variation of .

Now, after this approximate one-page crash course in the Ginzburg-Landau theory of superconductivity, we will move on to considering Josephson junctions.

©u© ¦\0 `n 0q\ nj a«jH§_nj

In 1962 Brian Josephson made the prediction, using BCS-theory, that a supercurrent I should flow between two superconducting electrodes separated by a thin non-superconducting layer [2]. He found that

$$I = I_c \sin(\phi_L \quad \phi_R) = I_c \sin(\quad \phi); \tag{2.8}$$

where the critical current I_c is the maximum current the junction can support, and ϕ_L and ϕ_R are the phases of the left and the right superconducting electrode, respectively. In the second equality we used the notation $\phi = \phi_L \quad \phi_R$. Josephson further predicted that if a voltage difference V was held over the junction, the phase difference would evolve as

$$\frac{d(\quad \phi)}{dt} = \frac{2eV}{\sim}: \tag{2.9}$$

Equations (2.8) and (2.9) can in fact be understood from GL-theory [2, 12]. Let us first derive (2.8). Consider a Josephson junction with a distance L between the two electrodes and choose the phase on one superconductor to be 0 and at the other to be ϕ. Now, consider the Ginzburg-Landau equation (2.7). We can write $f(x) = 1$ if $x \quad 0$ and $f(x) = e^i \quad$ if $x \quad L$. For $x\ 2\ [0; L]$ we have $f(x) \quad e^{i\ (x)}$, where $\phi(x)\ 2\ [0; \quad \phi]$. Then we can approximate:

$$\frac{d^2 f}{dx^2} \quad \frac{f(x + L) \quad 2f(x) + f(x \quad L)}{L^2} = \frac{e^i \qquad 2e^{i\ (x)} + 1}{L^2} \quad \frac{f}{L^2}: \tag{2.10}$$

Since in our case L , we see that the first term in (2.7) is dominating and the other terms can be neglected, unless $\phi = 0$ in which the solution is trivial $f \quad 1$. Hence, we get the equation $\frac{d^2 f}{dx^2} = 0$ which together with the boundary conditions yields the solution

$$f(x) = (1 \quad x=L) + (x=L)e^i \quad : \tag{2.11}$$

Inserting (2.11) into the Ginzburg-Landau equation (2.5) with $A = 0$ then yields the Josephson relation (2.8) where we identify $I_c = \frac{2e\sim j \ _1 j^2 A}{m \ L}$, where A is the cross-sectional area of the bridge.

Let us now derive equation the second Josephson relation, i.e. (2.9). The free energy stored in the junction can be found by (2.2), where we again are neglecting the $a(T)$ and $b(T)$ terms:

$$F = F_s \quad F_n = A \int_0^L \frac{\sim^2}{2m} j r \quad j^2 \, dx = \frac{I_c \sim}{2e}(1 \quad \cos \quad \phi) = E_J(1 \quad \cos \quad \phi); \quad (2.12)$$

where we have defined the Josephson energy $E_J \quad \frac{I_c \sim}{2e} = \frac{I_c \ 0}{2}$ where $\ 0$ is the magnetic flux quantum. Now, assume that the free energy in the junction varies only because of a change in the supercurrent I. Using the definition of electrical power, we can write

$$\frac{d \ F}{dt} = IV; \quad (2.13)$$

which means

$$\frac{@ \ F}{@ \ \phi}\frac{d \ \phi}{dt} = IV = V I_c \sin \quad \phi \quad) \quad \frac{d \ \phi}{dt} = \frac{I_c}{E_J}V = \frac{2e}{\sim}V; \quad (2.14)$$

which is precisely equation (2.9).

©u©uo W9«X0 _j®9}_9j§ q\9 0

In the preceding considerations, we have used the phase difference ϕ. However, this quantity is not gauge invariant, and cannot in general determine the gauge invariant quantity I [2]. The remedy for this is to replace ϕ with the X9«X0 _j®9}_9j§ q\9 0 L_¸0}0jH0 , which turns out to be

$$\phi \quad \frac{2}{\ 0} \int \mathbf{A} \ ds; \quad (2.15)$$

where the integral goes from one of the superconducting electrodes to the other.

©u©u© ¦ \0 | G~` h nL0e 9jL q\9 0 e_q

In practice, to get a complete description of the Josephson junction, one must take capacitive effects into consideration, since the system consists of two superconducting surfaces facing each other. Also, the possibility of tunneling of quasi-particles across the junction might lead to a finite resistance. The model that takes these effects into account is called the }0 _ §_®0e´ 9jL H9q9H_§_®0e´ \«j§0L a«jH§_nj (RCSJ)

hnL0e [1, 2, 12], see figure 2.1b. By equating the total current I to the currents in the three channels, we can write down the following equation:

$$I = I_J + I_R + I_C = I_c \sin \quad + \frac{V}{R} + C\frac{dV}{dt}: \tag{2.16}$$

For low voltages and low temperatures, the contribution from the tunneling of quasi-particle becomes negligible. For our purposes, we will therefore let $R \; ! \; 1$. Now, using the Josephson relation (2.9), we can rewrite (2.16) as:

$$I = I_c \sin \quad + \frac{\sim C}{2e}\frac{d^2}{dt^2}: \tag{2.17}$$

Multiplying both sides with $\sim=(2e)$, we see that this equation describes a "phase particle" with "mass" $(\sim=2e)^2C$ moving in the direction in the effective potential

$$U(\;) = \quad E_J \cos \quad \frac{\sim I}{2e} \; : \tag{2.18}$$

Due to its shape, $U(\;)$ is called the §_e§0L °9 \@n9}L qn§0j§_9e, see figure 2.1a.

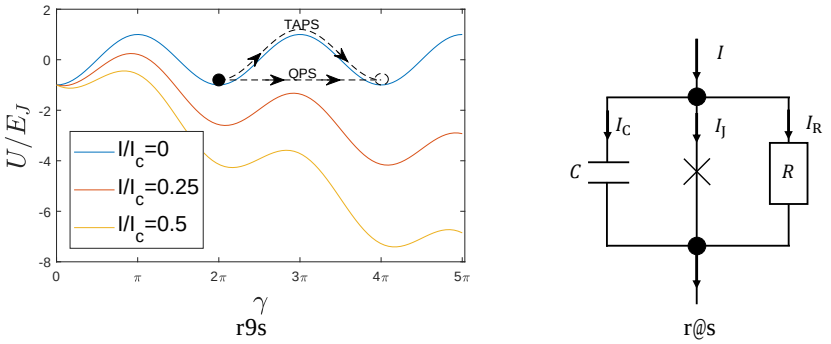

Figure 2.1: (a) The tilted washboard potential for different values of $I=I_c$. (b) An illustration of the RCSJ model.

Now, for low or zero bias current, equation (2.17) can be rewritten as

$$0 = I_c \quad + \frac{\sim C}{2e}\frac{d^2}{dt^2}: \tag{2.19}$$

From this equation we can identity the frequency with which the phase point oscillates back and forth. This is called the qe9 h9 T}0x«0jH´ $!_p$ and is found as

$$!_p = \quad \sqrt{\frac{2eI_c}{\sim C}}: \tag{2.20}$$

As is illustrated in figure 2.1a, the value of the phase can jump by a value of 2 due to either thermal or quantum fluctuations[o]. These phenomena are called §\0}h9ee´ 9H§_®9§0L q\9 0 e_q (TAPS) and x«9j§«h q\9 0 e_q (QPS), respectively. From the Josephson relation (2.9) we see that a change in phase indicates a voltage drop. Phase slips can be divided into two types: Hn\0}0j§ (quantum) phase slips and _jHn\0}0j§ phase slips.

Coherent phase slips are exactly dual to the DC Josephson effect; whereas the latter is a coherent transfer of electrons between two superconducting electrodes, the former is a coherent transfer of magnetic fluxes (or vortices) across a superconducting wire [14, 15]. A superconducting wire can simplified be seen as a chain of Josephson junctions [16]. Coherent phase slips are responsible for the Coulomb blockade state in a Josephson junction, where electron transport is blocked due to Coulomb repulsion.

Incoherent phase slips are dissipative, meaning that if a supercurrent flows through a chain of Josephson junctions then the phase slip is associated with the dissipation of electromagnetic energy [14]. Incoherent phase slips are the cause of the observed residual resistance in superconducting nanowires when the temperature is below the critical temperature [16].

Let us first consider TAPS. As illustrated in figure 2.1a, these occur when thermal fluctuations give the phase particle a push over a hump of the cosine potential. The transition rate can for thermally activated phase slips can be computed using Arrhenius law [16, 17]:

$$= \quad e \quad ^{F=T}; \tag{2.21}$$

where F is the free energy barrier for a phase slip of 2 and is the attempt frequency. If no current flows through the junction, meaning that $F = 2E_J$, and if R is large and T small in the RCSJ model, we can set $= !_p$. We see that TAPS decreases exponentially with decreasing temperature, and for low enough temperatures, the frequency of QPS should supersede that of TAPS.

The effects of phase slips in Josephson junctions will be considered in further detail in sections 2.6-2.7.

©u¨ 8 L_ _q9§_®0 x«9j§«h q\9 0 §}9j _§_nj

When studying solid state devices, it is important to keep in mind that macroscopic systems always interact with the environment. The constant exchange of energy with the environment leads to L_ _q9§_nj, meaning a transfer of energy from the system to the environment. The role of dissipative couplings for macroscopic systems was pointed out by Caldeira and Leggett (CL) [8]. More specifically, they studied how dissipation to the environment affects quantum tunneling between a

[o] [n°0®0}J §\0 q\9 0 Ln0 jn§ Ÿ°_jL «qŸ 9 9 §_X\§0j_jX \0e_²u ^j §09LJ §\0 q\9 0 _ 9 Hn h q9H§ ®9}_9@e0J h09j_jX _§ \9 q0}_nL_H @n«jL9}´ HnjL_§_nj E©J o¨Fu

meta-stable state into a continuum. As a basis in their study, they considered the quasi-classical equation of motion

$$M\ddot{q} + \dot{q} + \frac{@V}{@q} = F_{\text{ext}}; \tag{2.22}$$

where q is some coordinate, M is its associated mass, $V(q)$ is the potential with a meta-stable minimum, F_{ext} is an external force, and is a phenomenological friction coefficient. The power dissipated from the system is $\dot{q}^2$. Importantly, we see that (2.22) is exactly (2.16) (multiplied with $\sim=(2e)$) if we identify $q \; ! \;$, $M \; ! \; C(\sim=2e)^2$, $\; ! \; \frac{1}{R}(\sim=2e)^2$, $V \; ! \; U(\;)$ and $F_{\text{ext}} \; ! \; 0$.

CL modeled the environment as an infinite reservoir of harmonic oscillators and argued that a general macroscopic system, including the environment and the interaction between the system and the environment, can be described by (2.22). They then proceeded by estimating the tunneling rate and their discovery was that the tunneling rate *L0H}09 0* with *_jH}09 _jX* dissipation.

Inspired by this, Schmid [9] and Bulgadaev [10] further investigated the effect for the case of a periodic potential, such as the washboard potential in the RCSJ-model. Their studies led to the conclusion that a Josephson junction can undergo a *L_ _q9§_®0 x«9j§«h q\9 0 §}9j _§_nj* at zero temperature by tuning the variable across a critical value $_{\text{c}} = h=(2e)^2 \quad R_{\text{Q}}$ where R_{Q} is the quantum resistance. Above this value, the phase particle is localized, meaning that the correlation function decreases algebraically, and the junction is in a superconducting state. Below this value, the phase particle displays a diffusive behavior and the junction is in a metallic state. This transition is called the Schmid(-Bulgadaev) transition.

The Schmid transition for a single Josephson junction has been studied both experimentally (see e.g. the study by Pentillä et al. [18]) and with the use of Monte Carlo simulations (see e.g. the paper by Herrero and Zaikin [19]). In apparent contrast to theory, both studies found that the transition point did not only depended on the value but also on the value $K \quad \sqrt{E_{\text{J}}=E_{\text{C}}}$ of the Josephson junction, where $E_{\text{C}} = (2e)^2=C$. For small values of K, the transition was found to take place at $= R_{\text{Q}}$, but for larger values of K, the critical value $_{\text{c}}$ decreased. For large enough values of K, no phase transition at all was found; the junction was always in the superconducting state.

The two studies had different primary explanations for this deviation. Pentillä et al. explains the result with a finite accuracy of the voltage measurements. However, Herrero and Zaikin argues against this and declares that the experimental results are due to finite temperature effects, which turns the transition into a *H}n n®0}*, whose position depends on the both K and . For $T = 0$ they argued that this crossover becomes a phase transition.

Another study by Werner and Troyer [20] which used more efficient Monte Carlo simulations, confirmed that, for low temperatures and small values of K, the phase transition take place at $= R_{\text{Q}}$.[©]

[©] [n°0®0} §\0 0 _h«e9§_nj 9e n \n°0L §\9§ §\0 Hn}}0e9§_nj 0²qnj0j§ 9}0 L0q0jL0j§ nj *K* °_H\ h_X\§ h09j §\9§ 9 Hn h qe0§0 §\0n}0§_H9e «jL0} §9jL_jX _ h_ _jXu

©uV `n 0q\ nj a«jH§_nj H\9_j

As mentioned earlier, the aim of this thesis is to study one-dimensional Josephson junction arrays of different lengths. The ends of the chain are coupled to transmission lines, which plays the part of the dissipative coupling described in the previous section. See figure 2.2. No average current is allowed to flow through the system, however, a fluctuating voltage drop across the chain can be computed as $U = \int_1^{L_x} \mathbf{E}\ \mathrm{d}\mathbf{r} = (L_x - 1)\frac{\partial A}{\partial t}$ (in units of island spacing), where the spatial variations of the magnetic vector potential A are ignored due to the large speed of light.

The Hamiltonian of the Josephson chain is discussed in section 2.4.1. The calculation of the associated partition function is discussed in section 2.4.2. The fluctuating voltage drop is for simplicity ignored in 2.4.1 but is taken into consideration in 2.4.2.

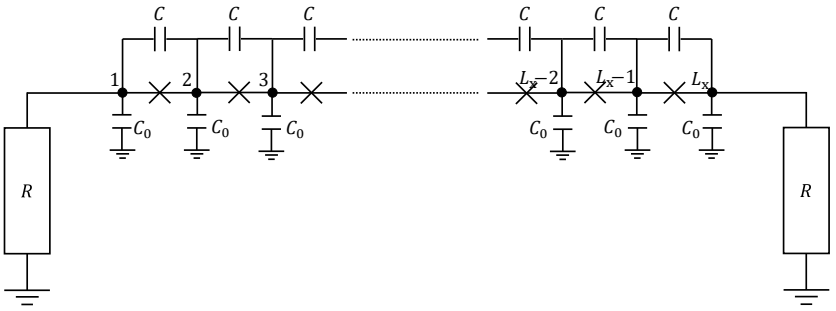

Figure 2.2: A Josephson chain with its ends coupled to transmission lines. This is the system this thesis is investigating.

©uVuo ¦\0 [9h_e§nj_9j

As is illustrated in figure 2.2, we will consider a Josephson junction chain with L_x superconducting islands with no applied current or voltage bias. The Hamiltonian for the Josephson chain can be split into two contributions: the potential energy stored in the junctions, and the electrostatic energy of each superconducting island due to both the inter-island capacitance C and the capacitance to ground C_0. The former contribution was found in section 2.2 and is simply given by $\sum_j E_J \cos(\ _j)$ where j represents a summation over a«jH§_nj ($j = 1; 2; :::; L_x - 1$).

The latter contribution can be expressed either in terms of voltages or charges. It will be convenient in section 2.4.2 to be able to do both. Let us denote the charge and electrostatic potential on island i as Q_i and V_i, respectively. Using vector notation, these are related as $\mathbf{Q} = \mathbf{C}\mathbf{V}$ where $\mathbf{C}$ is the capacitance matrix for the system. To find $\mathbf{C}$, let us first be a bit more general and denote the capacitance

between two islands i and i^0 as $c_{i;i^0}$ (for our system we have of course that $c_{i;i^0} = C(\ _{i;i^0+1} + \ _{i;i^0\ 1})$). Considering the contributions from all capacitors connected to an island, we find that

$$Q_i = C_0 V_i + \sum_{i^0=1;i^0\neq i}^{L_x} c_{i;i^0}(V_i - V_{i^0}) = V_i \Big[C_0 + \sum_{i^0=1;i^0\neq i}^{L_x} c_{i;i^0}\Big] - \sum_{i^0=1;i^0\neq i}^{L_x} c_{i;i^0} V_{i^0}: \quad (2.23)$$

From this, we can determine the elements $C_{i;i^0}$ of $\mathbf{C}$ as $C_{i;i^0} = -\sum_{i^0=1;i^0\neq i}^{L_x} c_{i;i^0}$ if $i \neq i^0$ and $C_{i;i} = C_0 + \sum_{i^0=1;i^0\neq i}^{L_x} c_{i;i^0}$. For our system, the capacitance matrix can therefore be found as

$$C_{i;i^0} = \begin{cases} C_0 + C & \text{if } i = i^0 \in \{1; L_x\} \\ C_0 + 2C & i = i^0 \notin \{1; L_x\} \\ -C & \text{if } |i - i^0| = 1 \\ 0 & \text{otherwise} \end{cases}; \quad (2.24)$$

or if one prefers, $C_{i;i^0} = (C_0 + 2C)\ _{i;i^0} - C(\ _{i;i^0+1} + \ _{i;i^0\ 1} + \ _{i;1\ \ i^0;1} + \ _{i;L_x\ \ i^0;L_x})$:

Now, the energy stored in the electric field E in a parallel plate capacitor with distance d between the plates and capacitance c is $\frac{1}{2}cd^2E^2 = \frac{1}{2}cV^2$, where V is the voltage between the plates. The total electrostatic energy E_{ch} of the superconducting islands can therefore be written as:

$$E_{\text{ch}} = \sum_i \frac{1}{2}C_0 V_i^2 + \sum_j \frac{1}{2}C(V_{j+1} - V_j)^2 = \sum_{i;i^0} \frac{1}{2}V_i C_{i;i^0} V_{i^0} = \sum_{i;i^0} \frac{1}{2}Q_i C^{-1}_{i;i^0} Q_{i^0} \quad (2.25)$$

where the indices i and i^0 denotes summation over $\_ \in \{9jL$ and j denotes the summation over $ɑ«jH§_nj$. This notation will be used throughout the thesis.

Now we can write down the Hamiltonian for the Josephson chain. Upon quantization, and denoting the number of Cooper pair on island i as $n_i = Q_i/(-2e)$, the Hamiltonian is the following:

$$\hat{H}_{QPM} = \frac{(2e)^2}{2} \sum_{i;i^0} (\hat{n}_i - n_{x;i}) C^{-1}_{i;i^0} (\hat{n}_{i^0} - n_{x;i^0}) - E_J \sum_j \cos(\hat{\phi}_{j+1} - \hat{\phi}_j - A_j); \quad (2.26)$$

where $\hat{n}_i = -i\frac{d}{d}$ and $\hat{\phi}_i$ are the number and phase operator for the Cooper pairs on island i, respectively, which obey the commutation relation $[\hat{\phi}_i; \hat{n}_{i^0}] = i\ _{i;i^0}$. For completeness, we have added an "offset charge" $n_{x;i}$ which can be caused by an applied external electric field or some trapped charges which breaks the symmetry of positive and negative charges [4]. However, this offset charge will be neglected for the rest of this thesis. A_j is the integral of the vector potential across the junction:

$$A_j = \frac{2}{\ _0} \int_j^{j+1} \mathbf{A} \cdot d\mathbf{s}: \quad (2.27)$$

The two different terms in (2.26) favor the system to be in different ground states [4]. The first favors charge localization and the second favors phase coherence. This

can be seen using the second Josephson relation (2.9) (which can be found for the operator using the Heisenberg equation of motion):

$$\frac{d\hat{\phi}_i}{dt} = \frac{2e}{\sim}\hat{n}_i: \tag{2.28}$$

We see that a constant charge means large fluctuations in the phase. On the other hand, we know from the uncertainty principle $\phi_i \quad n_i \quad 1$ that phase coherence means large fluctuations in the charge.

The strength ratio between the two terms can be described by $K \quad \sqrt{E_J=E_C}$ where $E_C = (2e)^2=C$. For $K \quad 1$ the Josephson junction chain should be in a superconducting state and for $K \quad 1$ it should be in an insulating state. We will call K the superconducting stiffness.

The Hamiltonian (2.26) is called the Quantum Phase Model (QPM). It is closely related to other Hamiltonians that appear in physics. In fact, an alternative way to derive it is from the general Bose-Hubbard Hamiltonian [4]. In the special case $C \; ! \; 0$, QPM can be mapped onto the XY-model (see section 2.6), and adding the condition $A_j = 0$, (2.26) is identical to the quantum rotor model (see e.g. [21]).

Lastly, we will write the electrostatic Hamiltonian in a slightly different way;

$$\hat{H}_{\text{ch}} = \frac{(2e)^2}{2}\sum_{i;i^0}\hat{n}_i C^{-1}_{i;i^0}\hat{n}_{i^0} = \frac{E_{C_0}}{2}\sum_{i;i^0}\hat{n}_i G_{i;i^0}\hat{n}_{i^0}; \tag{2.29}$$

where we have defined $G_{i;i^0} \quad C_0 C^{-1}_{i;i^0}$ and $E_{C_0} \quad (2e)^2=C_0$. For $C_{i;i^0}$ given by (2.24), $G_{i;i^0}$ is given by (see appendix A)

$$G_{i;i^0} = \frac{1}{L_x} + G^0(i \quad i^0) + G^0(i + i^0 + 1) \;; \tag{2.30}$$

where

$$G^0(x) = \frac{1}{L_x}\sum_{n=1}^{L_x-1}\frac{\cos\frac{n}{L_x}x}{1 + 4\ ^2\sin^2\frac{n}{2L_x}}; \tag{2.31}$$

and $\sqrt{C=C_0}$ is the charge screening length (in units of island spacing). Large and small values of corresponds to a long-range and a short-range Coulomb interaction, respectively. In practical experiments, the value for is often $' 10$ [22]. The advantage with this formulation for the electrostatic Hamiltonian is that we in the simulations can work with a single value instead of choosing two values C and C_0.

©uVu© p9}§_§_nj T«jH§_nj

In this section we will use the Hamiltonian operator found in the previous chapter to express the partition function of the system with a path integral formulation. These calculations will lead to a mapping from the 1-dimensional quantum system to a

(1+1)-dimensional classical system, where the extra dimension extends in imaginary time. The calculations found here are largely based on those that can be found in [21, 23]. The main result of the section is equation (2.63) which will form the basis for the Monte Carlo method described in section 3.2.

From the previous section, we have that the Hamiltonian of the Josephson chain is

$$\hat{H}_{\mathrm{QPM}} = \hat{H}_{\mathrm{ch}} + \hat{H}_{\mathrm{J}};$$
$$\hat{H}_{\mathrm{ch}} = \frac{E_{C_0}}{2} \sum_{i;i'} \hat{n}_i G_{i;i'} \hat{n}_{i'}; \quad \hat{H}_{\mathrm{J}} = E_{\mathrm{J}} \sum_j \cos(r_x \hat{\phi}_j - A_j); \tag{2.32}$$

where $r_x \hat{\phi}_j = \hat{\phi}_{j+1} - \hat{\phi}_x$.

Let us first consider a general system governed by a Hamiltonian H. We know from quantum statistical mechanics that the partition function Z is $Z = \mathrm{Tr}\, e^{-\beta \hat{H}}$, where $\beta = 1/T$.[¨] We see that this can be written in terms of the time evolution operator $e^{-i\hat{H}T}$ if we put $T = -i\beta$. Writing the partition function as $Z = \sum_n \langle n|e^{-\beta \hat{H}}|n\rangle$, where $\{|n\rangle\}$ is a complete set of states, we can interpret the partition function as a sum of imaginary-time transition amplitudes for the system to start in a state $|n\rangle$ and return to the same state after an imaginary time interval $-i\beta$. Doing a Trotter decomposition, i.e. discretizing the imaginary time interval $[0; -i\beta]$ into L slices, each with width ε such that $L\varepsilon = -i\beta$, the partition function becomes

$$Z = \mathrm{Tr}\, e^{-\beta \hat{H}} = \lim_{\varepsilon \to 0} \mathrm{Tr}\,(e^{-\varepsilon \hat{H}})^L : \tag{2.33}$$

Let us now go back to our system. We have a complete set of states $|\{\phi(\tau_k)\}\rangle = \bigotimes_{i=1}^{L_x} |\phi_i(\tau_k)\rangle$ which describes the phase of the islands $i = 1; \ldots; L_x$ at time slice k. By inserting a completeness relation between each factor $e^{-\varepsilon \hat{H}_{\mathrm{QPM}}}$ in (2.33), the partition function can be written as:

$$\begin{aligned} Z &= \lim_{\varepsilon \to 0} \int \frac{d\phi_0}{2} \langle \{\phi(\tau_0)\}| (e^{-\varepsilon \hat{H}_{\mathrm{QPM}}})^L |\{\phi(\tau_0)\}\rangle \\ &= \lim_{\varepsilon \to 0} \int \frac{d\phi_0}{2} \frac{d\phi_1}{2} \cdots \frac{d\phi_{L-1}}{2} \langle \{\phi(\tau_0)\}| e^{-\varepsilon \hat{H}_{\mathrm{QPM}}} |\{\phi(\tau_{L-1})\}\rangle \\ &\quad \langle \{\phi(\tau_{L-1})\}| e^{-\varepsilon \hat{H}_{\mathrm{QPM}}} |\{\phi(\tau_{L-2})\}\rangle \cdots \\ &\quad \langle \{\phi(\tau_2)\}| e^{-\varepsilon \hat{H}_{\mathrm{QPM}}} |\{\phi(\tau_1)\}\rangle \langle \{\phi(\tau_1)\}| e^{-\varepsilon \hat{H}_{\mathrm{QPM}}} |\{\phi(\tau_0)\}\rangle : \end{aligned} \tag{2.34}$$

If ε is small, this can more compactly can be written as

$$Z \approx \int D\{\phi(\tau)\} \prod_{k=0}^{L-1} \langle \{\phi(\tau_{k+1})\}| e^{-\varepsilon \hat{H}_{\mathrm{QPM}}} |\{\phi(\tau_k)\}\rangle ; \tag{2.35}$$

[¨] 0 « 0 «j_§ ° \0}0 $k_{\mathrm{B}} = \sim = 1$ɯ

where we have imposed periodic boundary conditions in the imaginary time direction: $|\phi(0)\rangle = |\phi(L)\rangle$. Now, for small values of $\Delta\tau$ we can approximate $e^{-\Delta\tau(\hat{H}_{QPM}+\hat{H}_{ch}+\hat{H}_J)} \approx e^{-\Delta\tau\hat{H}_{QPM}} e^{-\Delta\tau\hat{H}_{ch}} e^{-\Delta\tau\hat{H}_J}$. Therefore, (2.35) becomes

$$\begin{aligned} Z &= \int D[\phi(\tau)] \prod_{k=0}^{L-1} \langle\phi(\tau_{k+1})|e^{-\Delta\tau\hat{H}_{ch}} e^{-\Delta\tau\hat{H}_J}|\phi(\tau_k)\rangle \\ &= \int D[\phi(\tau)] \prod_{k=0}^{L-1} e^{-\Delta\tau E_J \sum_j \cos(\nabla_\tau \phi_j - A_j)} \langle\phi(\tau_{k+1})|e^{-\Delta\tau\hat{H}_{ch}}|\phi(\tau_k)\rangle; \end{aligned} \tag{2.36}$$

where we used that $|\phi(\tau_k)\rangle$ are eigenstates of $\hat{H}_J$. To simplify the notation, we have used $\phi_i = \phi_i(\tau_k)$ in the exponent. Both notations will be used from here on. We can consider the electrostatic part of each site separately, since the $\hat{n}_x$ operators commute for different sites. We introduce eigenstates $|n(\tau_k)\rangle$ of the $\hat{n}_i$ operators with eigenvalues $n_i \in \mathbb{Z}$. We have that $\langle\phi_i(\tau_k)|n_i(\tau_{k'})\rangle = e^{in_i(\tau_k)\phi_i(\tau_{k'})}$. Inserting this complete set of states yields

$$\begin{aligned} &\langle\phi(\tau_{k+1})|e^{-\Delta\tau\hat{H}_{ch}}|\phi(\tau_k)\rangle \\ &= \sum_{\{n(\tau_k)\}} \prod_i e^{-\frac{\Delta\tau E_{C_0}}{2}\sum_{i',i''} n_{i'} G_{i',i''} n_{i''}} \langle\phi_i(\tau_{k+1})|n_i(\tau_k)\rangle\langle\phi_i(\tau_k)|n_i(\tau_k)\rangle \\ &= \sum_{\{n(\tau_k)\}} e^{-\frac{\Delta\tau E_{C_0}}{2}\sum_{i,i'} n_i G_{i,i'} n_{i'} - i\sum_i n_i \nabla_\tau \phi_i}; \end{aligned} \tag{2.37}$$

where we have used the notation $\nabla_\tau \phi_i = \phi_i(\tau_{k+1}) - \phi_i(\tau_k)$. Combining (2.36) and (2.37), the partition function can thus be written as

$$Z = \sum_{\{n_i\}} \int D[\phi(\tau)] e^{-S}; \tag{2.38}$$

where

$$\begin{aligned} S = \sum \Big(& E_J \sum_j \cos(\nabla_\tau \phi_j - A_j) \\ & + \frac{E_{C_0}}{2} \sum_{i,i'} n_i G_{i,i'} n_{i'} - i\sum_i n_i \nabla_\tau \phi_i \Big); \end{aligned} \tag{2.39}$$

and where S is the *N«He_L09j 9H§_nj*.

We end this section by making a short summary of what we have done so far; a path integral formulation has been used where the imaginary time was discretized into slices to obtain a partition function on a space-time lattice with periodic boundary conditions in the time direction. The discretization in the spatial direction is made up by the superconducting islands. In the following section, it will be useful to have a picture of such a space-time lattice in mind, see e.g. figure 3.1.

^jHe«L_jX ¼«H§«9§_nj _j h9XjO§_H qn§Oj§_9e

As mentioned, we have so far only regarded the magnetic potential $\mathbf{A}$ as an external parameter. However, it is important to also consider fluctuations in $\mathbf{A}$ [23, 24]. To do this, let us first rewrite (2.39) in terms of electric potentials:

$$S = \sum_i \Big(\sum_j \Big[i n_i \, r_\tau \phi_i + \frac{1}{2} C_0 V_i^2 \Big] + \sum_j \Big[\frac{1}{2} C \, (V_{j+1,\tau} - V_j)^2 - E_J \cos(r_x \phi_j - A) \Big] \Big) \; . \tag{2.40}$$

The electric field in real time is computed as $\mathbf{E} = -\nabla V - \partial_t \mathbf{A}$. In the procedure where we to rotate to imaginary time, this relation will be transformed to $\mathbf{E} = -\nabla V + \partial_\tau \mathbf{A}$. In the action (2.40) we will then do the replacement:

$$\begin{aligned} r_x V_j = (V_{j+1,\tau} - V_j) \to \int_j^{j+1} \mathbf{E} \cdot d\mathbf{r} &= -r_x V_{x,\tau} + \int_j^{j+1} \frac{\partial \mathbf{A}}{\partial \tau} \cdot d\mathbf{r} \\ &= -r_x V_{j,\tau} + \frac{1}{2e} r \cdot A \; , \end{aligned} \tag{2.41}$$

where we in the last equality discretized the derivative, used (2.27), and neglected spatial variations in A. Doing this replacement and adding an important potential term $\sum_i 2eiV_i$, the partition function and action become, after some simplifications[V]

$$Z = \sum_{\{n_i\}} \int D[\phi(\tau)] \int D[V_{x,\tau}] \int D[A_\tau] \, e^{-S} ; \tag{2.42}$$

$$S = S_\mathrm{i} + S_\mathrm{j} ; \tag{2.43}$$

$$S_\mathrm{i} = \sum_{i,i'} \Big(\sum_i \Big[\frac{1}{2} V_i \, C_{i,i'} V_{i'} - i n_i \, r_\tau \phi_i + 2ein_i \, V_i \Big] - \frac{C(r \cdot A)}{2e} (V_{L_x,\tau} - V_{1,\tau}) \Big) \; ; \tag{2.44}$$

$$S_\mathrm{j} = \sum_j \Big(\frac{C(L_x - 1)}{2} \frac{(r \cdot A)^2}{(2e)^2} - E_J \cos(r_x \phi_j - A) \Big) \; . \tag{2.45}$$

Our goal is now to simplify the partition function until we arrive to a result that can be used in Monte Carlo simulations.

Let us first consider the effect of the integration over the phase for each point on the space-time lattice. Let I denote the contribution of the integral over $\{\phi_i\}$. To

[V] ¦ \0 0 }OqeHO h Oj§ 9}O a« § He9 _H9e 9j9enX nT §\0 h_j_h 9e Hn«qe_jXu

simplify the cosine term in the action, we will use the Jacobi–Anger expansion which can be written as $e^{K\cos} = \sum_{m=-1}^{1} I_m(K)e^{im} = \sum_{m=-1}^{1} e^{\log[I_m(K)]}e^{im}$ where I_m is the modified Bessel function of the first kind. For small values of K, only the terms with $m = 0;\ 1$ will contribute significantly. Doing this approximation, I can be computed as

$$I \quad \int Df\phi(\ )g e^{\sum_{J}\sum_{j}\cos(r_{x\ j}\ A_j)+i\sum_{i}n_i\ r_{\ i}} \tag{2.46}$$

$$= \int Df\phi(\ )g \sum_{fm_j g} e^{\sum_{i}\ E_J\sum_{j}m_j\ (r_{x\ j}\ A_j)+\sum_{j}\log[I_{m_j}(\ E_J)]} \tag{2.47}$$

$$e^{\sum_{i}\sum_{i}n_i\ r_{\ i}};$$

where $\sum_{fm_i g} = \sum_{m_1(\ 0)}\sum_{m_1(\ 1)}\cdots\sum_{m_1(\ L_{\ 1})}\sum_{m_2(\ 0)}\cdots\sum_{m_{L_x}(\ L_{\ 1})}$ is a sum over an integer $m_i(\ _k)$ for all space-time lattice points. Now, using a shift of indices and the periodicity in the time direction, we have that

$$i\sum_{j}\Big[\sum_{}m_j\ r_x\phi_j + \sum_{i}n_i\ r\ \phi_x = i\sum_{i}\Big[\sum_{}\phi_i\ (\overline{r}\ n_i + \overline{r}_x m_i) + \phi_{1;\ m_{0;}}\ \ \phi_{L_x;\ m_{L_x;}}\Big]; \tag{2.48}$$

where $\overline{r}\ n_x = n_x(\ _k)\ \ n_x(\ _{k\ 1})$ and $\overline{r}_x m_x = m_x(\ _k)\ \ m_{x\ 1}(\ _k)$. For compactness, let us include the "extra terms" $m_{0;}$ and $m_{L_x;}$ terms in the symbol $\overline{r}^{+}_{x}$, i.e.

$$\overline{r}^{+}_{x}\ m_{i;} = \overline{r}_x m_{i;} + {}_{i\ 1;0}m_{0;}\ \ {}_{i;L_x}m_{L_x;}: \tag{2.49}$$

This means that we can write

$$I = \int Df\phi(\ )g \sum_{fm_j g} e^{i\sum_{i}\ _i\ (\overline{r}\ n_i\ +\overline{r}^{+}_{x}m_i)} e^{i\sum_{j}\ A_j\ m_j\ +i\log[I_{m_j}(\ E_J)]} \tag{2.50}$$

$$= \sum_{fm_j g} e^{i\sum_{j}\sum\ A_j\ m_j\ +i\log[I_{m_j}(\ E_J)]} \int Df\phi(\ )g e^{i\sum_{i}\ _i\ (\overline{r}\ n_i\ +\overline{r}^{+}_{x}m_i)}: \tag{2.51}$$

The integral in (2.51) yields a product of Kronecker deltas, one for each space-time point in the lattice:

$$\int Df\phi(\ )g e^{i\sum_{i}\sum\ _i\ (\overline{r}\ n_i\ +\overline{r}^{+}_{x}m_i)} = \prod_{i;}\ {}_{0;\overline{r}^{+}_{x}m_i\ +\overline{r}\ n_i}: \tag{2.52}$$

The physical interpretation of the m_i -variables is that they are the currents from island i to $i+1$. $m_{0;}$ and $m_{L_x;}$ are currents that are entering and leaving the space-time lattice. Since n_i is the number of Cooper pairs on island i, the product of Kronecker deltas above describes current conservation.

Now, let us consider the first factor in (2.51). For $E_J \;!\; 0$ and $m_j = 0;\ \pm 1$, which should be true for $\;!\; 0$, we can approximate $\log[I_{m_j}(E_J)]$ $\log\frac{I_1(E_J)}{I_0(E_J)}(m_j)^2 + const.$ For compactness, let us also define a variable

$$J_i = (m_i\ ;n_i); \tag{2.53}$$

i.e. $J_i^x = m_i$ and $J_i = n_i$. We will call J_i^x and J_i link-currents. Using the result for I, the partition function can be written as

$$Z = \sum_{\{J_i\}} \int Df V_x;\ g \int DfA\ ge^{\ S_{0;\overline{r}^+ J}}; \tag{2.54}$$

where $\overline{r}^+ J = \overline{r}_x^+ m_i + \overline{r}\ n_i$ and

$$S_i = \sum_i \Big(\sum_{i^0} \frac{1}{2} V_i\ C_{i;i^0} V_{i^0} + 2ei J_i\ V_i \Big) - \frac{C(r\ A)}{2e}(V_{L_x} - V_1)\ ; \tag{2.55}$$

$$S_j = \sum_j \Big(\frac{C(L_x\ 1)}{2\ (2e)^2}(r\ A)^2 + \sum_j \Big[iJ_j^x\ A - \log\frac{I_1(E_J)}{I_0(E_J)} \Big]\ (J_j^x)^2 \Big)\ : \tag{2.56}$$

Now, let us introduce a dimensionless charge field q_x such that

$$J_x = (J_x^x\ ;J_x) = (\overline{r}\ q_x\ ;\ \overline{r}_x^+ q_x\ ): \tag{2.57}$$

We see that this automatically fulfills the condition $0 = \overline{r}^+ J_x = \overline{r}_x^+ \overline{r}\ q_x - \overline{r}\ \overline{r}_x^+ q_x$ [23, 24]. What is the interpretation of q_x in the lattice? To see this, let us first introduce an operator R which rotates each vector in a vector field 90° counter-clockwise. Therefore, $RJ_x = (-J_{x;}\ ;J_{x;}^x)$. We see that $\overline{r}^+ (RJ_x) = \overline{r}^+ J_x = 0$.[U] Hence, we can write $RJ_x = \overline{r}^+ q_x$ where q_x is a scalar potential defined uniquely up to an additive constant. RJ_x then points orthogonal to the level curves of q_x, and J_x constitutes contours of constant height. Each time we "cross" a link-current, the q_x will change with an integer value. See figure 3.1.

Now, rewriting J_i^x as $\overline{r}\ q_i$ and using $\sum_p (\overline{r}\ q_x)A = \sum_p q_x\ r\ A$, (2.56) can then be rewritten as

$$S_j = \sum_j \Big(\frac{C(L_x\ 1)}{2\ (2e)^2}(r\ A)^2 - \sum_j \Big[iq_j\ (r\ A) + \log\frac{I_1(E_J)}{I_0(E_J)} \Big]\ (J_j^x)^2 \Big)\ : \tag{2.58}$$

Now, let us do the integration over $\int fV_i\ g$. We will use the standard result for Gaussian integrals: $\int dx \exp(-\frac{1}{2}xAx + iJx) \;/\; \exp(-\frac{1}{2}JA^{-1}J)$. To get the

[U] ? ´ 0x«9§_jX 9 ®OH§n} 9jL 9 H9e9} §n 0 °0 h09j §\9§ 09H\ Hn h qn j0j§ _j §\0 ®OH§n} _ ·u

integrand on a fitting form, let us first denote $_i$ $i\frac{(r\ A\ )C}{2e}(\ _{L_x;i}$ $_{1;i})$. Then S_i can be written as

$$S_\mathrm{i} = \sum_{i;i'} \frac{1}{2} V_i\ C_{i;i'} V_{i'} \sum_i iV_{i;}\ (\ 2eJ_i\ \ _i)\ :\tag{2.59}$$

When the integration is performed, S_i will be transformed to

$$\begin{aligned} S_\mathrm{i} &= \sum_{i;i'} \frac{1}{2}(\ 2eJ_i\ \ _i)C^{-1}_{i;i'}(\ 2eJ_{i'}\ \ _{i'}) \\ &= \sum_{i;i'} \frac{(2e)^2}{2} J_i\ C^{-1}_{i;i'} J_{i'}\ + i(r\ A\ )C \sum_i J_i\ (C^{-1}_{i;L_x}\ \ C^{-1}_{i;1}) \\ &\qquad \frac{C^2}{2\ \ (2e)^2}(r\ A\ )^2(C^{-1}_{L_x;L_x} + C^{-1}_{1;1}\ \ C^{-1}_{L_x;1}\ \ C^{-1}_{1;L_x})\ : \end{aligned}\tag{2.60}$$

Next, we will be doing the final integration over the vector potential. For this, we again use the same standard result for Gaussian integration.[£] Again, to get the integrand on the appropriate form, we gather the factors in front of the $i(r\ A\ )$ terms in S_i and S_j and call this Q , i.e.

$$\begin{aligned} Q &= \sum_j q_j\ \ C \sum_i J_i\ (C^{-1}_{i;L_x}\ \ C^{-1}_{i;1}) \\ &= \sum_j q_j\ \ {}^2 \sum_i J_i\ (G_{i;L_x}\ \ G_{i;1}): \end{aligned}\tag{2.61}$$

The constants in front of $(r\ A\ )^2{=}2$ can also they be gathered into another constant $(E_\mathrm{C}\ \ )^{-1}$, i.e.

$$\begin{aligned} (E_\mathrm{C}\ \ )^{-1}\ \ \frac{L_x\ \ 1}{E_\mathrm{C}}\ \ \frac{C^2}{(2e)^2}(C^{-1}_{L_x;L_x} + C^{-1}_{1;1}\ \ C^{-1}_{L_x;1}\ \ C^{-1}_{1;L_x}) \\ = \frac{E_\mathrm{C}}{(L_x\ \ 1)\ \ {}^2(G_{L_x;L_x} + G_{1;1}\ \ G_{1;L_x}\ \ G_{L_x;1})}\ \ !^{\ 1}\ \ : \end{aligned}\tag{2.62}$$

[£] ¦n Ln §\0 _j§0X}9§_njJ nj0 q0}Tn} h 9 «@ §_§«§_nj nT §\0 ®9}_9@e0 $A^0 = r\ A\ = A_{+1}\ A$ u ¦\0 }0 «e§_jX `9Hn@_9j °_eeJ L«0 §n §\0 e_j09} }0e9§_nj _q @0§°00j §\0 A^0I 9jL §\0 A I J nje´ X_®0 9j _}}0e0®9j§ Hnj §9j§ T9H§n}u

The integration over A then finally yields the expression

$$\boxed{\begin{aligned} Z &= \sum_{\{\mathbf{J}_i\}} e^{-(S_\mathbf{J}+S_Q)/k_B T}, \\ S_\mathbf{J} &= \sum_{\langle i,i'\rangle} \frac{E_{C_0}}{2} J_i G_{i,i'} J_{i'} - \log\left[\frac{I_1(E_J/k_B T)}{I_0(E_J/k_B T)}\right] \sum_j (J_j^x)^2, \\ S_Q &= \sum_i \frac{1}{2} E_C Q_i^2 . \end{aligned}} \qquad (2.63)$$

Equation (2.63) is the main result of this section. This expression of the partition function is the one used in the Monte Carlo simulations. However, in section 2.7, we will see that it will be useful to rewrite it in a different form. First, note that we can replace the summation over $\{\mathbf{J}_i\}$ with a summation over $\{q_x\}$. Next, using Poisson's summation formula,

$$\sum_{s=-\infty}^{+\infty} g(s) = \sum_{m=-\infty}^{+\infty} \int_{-1/2}^{1/2} d\theta\, g(\theta) e^{2\pi i m\theta}, \qquad (2.64)$$

where $g(s)$ is any function. Z in (2.63) can therefore be rewritten as

$$Z = \sum_{\{q_x\}} e^{-(S_\mathbf{J}+S_Q)/k_B T} = \sum_{\{v_x\}} \int D\{q_x\}\, e^{-(S_\mathbf{J}+S_Q)/k_B T} 2\pi i \sum_x q_x v_x , \qquad (2.65)$$

where the integer field v_x can take any value in Z. These fields represent vortices in the original phase model [23].

©uU ^j¼«OjHO nT §°n §}9j h_ _nj e_jO Hn«qeOL §n §\O `n Oq\ nj a«jH§_nj H\9_j

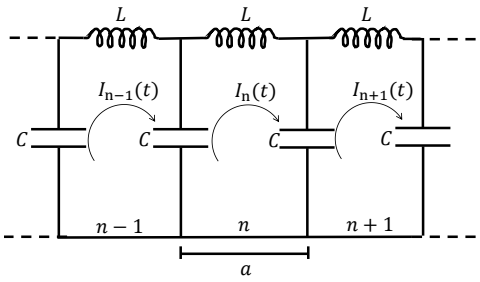

Figure 2.3: A transmission line modeled as a semi-infinite LC ladder. $I_n(t)$ is the loop current in the n:th section at time t.

In this section, we will investigate how the coupling of transmission lines to the ends of the Josephson chain will influence the system. These will be the dissipative couplings discussed in section 2.3. We will model each transmission line as a semi-infinite LC ladder, see figure 2.3, reaching from the ends of the Josephson chain to $x = \quad 1$.[¢]

We wish to first find the Lagrangian describing a transmission line. For this, we will follow the procedure found in [25]. Let us denote the integrated charge as $Q_n(t)$, i.e. the charge that has passed through the n:th inductor after time t ($Q_n(t) = \int_0^t I_n(s)\,ds$). If we consider the energy in the inductors as a kinetic energy and the energy stored in the capacitors as a potential energy, we can write the discrete Lagrangian as

$$L_T = \frac{1}{2}\sum_n L\left(\frac{@Q_n}{@t}\right)^2 \quad \sum_n \frac{1}{2C}[Q_{n+1}(t) \quad Q_n(t)]^2: \tag{2.66}$$

The continuous system is obtained by letting the spacing $a \;!\; 0$. The result is what one would expect from (2.66), and we get the Lagrangian density

$$L_T = \frac{1}{2}\, l \left(\frac{@Q}{@t}\right)^2 \quad \frac{1}{c}\left(\frac{@Q}{@x}\right)^2 ; \tag{2.67}$$

where l and c are the distributed inductance and capacitance, respectively. Using a coordinate system where the transmission line stretches between 0 and (minus-)infinity, and using $T = \quad i$ and $\quad = it$, we can write down the action of the

[¢] mj0 h_X\§ x«0 §_nj \n° 9 §}9j h_ _nj e_j0 h9L0 «q @´ q«}Oe´ }O9H§_®O OeO h0j§ H9j L_ _q9§O 0j0}X´u [n°O®O}J _jHO §\O §}9j h_ _nj]e_j0 _ 0h_]_j»j_§OJ 9 °9®O e9«jH\OL _j njO 0jL H9}}_O n¸ 0j0}X´ 9jL jO®O} }O§«}j u ¦_ 9}X« h0j§ _j®ne®O 9 H9}OT«e Hnj _LO}9§_nj nT §\O n}LO} nTe_h_§ Eo¨Fu

transmission line:

$$\begin{aligned} S_{\mathrm{T}} &= \int_0^T \mathrm{d}t \int_0^1 \mathrm{d}x \, \frac{1}{2}\left[l \left(\frac{@Q}{@t}\right)^2 - \frac{1}{c}\left(\frac{@Q}{@x}\right)^2 \right] \\ &= i \int_0^{} \mathrm{d} \int_0^1 \mathrm{d}x \, \frac{1}{2}\left[l \left(\frac{@Q}{@}\right)^2 + \frac{1}{c}\left(\frac{@Q}{@x}\right)^2 \right] = i S_{\mathrm{T}}^{\mathrm{E}}; \end{aligned} \tag{2.68}$$

where we have defined the Euclidean action as

$$S_{\mathrm{T}}^{\mathrm{E}} \int_0^{} \mathrm{d} \int_0^1 \mathrm{d}x \, \frac{1}{2}\left[l \left(\frac{@Q}{@}\right)^2 + \frac{1}{c}\left(\frac{@Q}{@x}\right)^2 \right]: \tag{2.69}$$

Integration by parts together with a substitution of variables $x^0 = {}^p\overline{c}x$, $^0 = = {}^p\overline{l}$ yields that

$$\begin{aligned} S_{\mathrm{T}}^{\mathrm{E}} &= \int_0^{p\overline{l}} \mathrm{d}^{\,0} \int_0^{} \mathrm{d}x^0 \frac{1}{2}\left[\sqrt{\frac{l}{c}} \left(\frac{@Q}{@^{\,0}}\right)^2 + \left(\frac{@Q}{@x^0}\right)^2 \right] = \\ &= \frac{1}{2}\sqrt{\frac{l}{c}} \int_0^{p\overline{l}} \mathrm{d}^{\,0} \int_0^{} \mathrm{d}x^0 \, (r^{\,0}Q) \cdot (r^{\,0}Q) \\ &= \frac{1}{2}\sqrt{\frac{l}{c}} \left[\int_S Q\, r^{\,0}Q \cdot \mathrm{d}S - \int Q\, r^{\,02}Q \, \mathrm{d}x^0 \mathrm{d}^{\,0} \right]; \end{aligned} \tag{2.70}$$

where S denotes the boundaries of the Euclidean space and $r^{\,0}Q = (@_{x^0}Q; @_{\,0}Q)$. Enforcing the condition that Q is periodic in imaginary time

$$Q(x;0) = Q(x; \ ); \tag{2.71}$$

and that the spatial derivative of the charge at the ends is zero[P]

$$@_x Q(x; \ )j_{x=0} = @_x Q(x; \ )j_{x=1} = 0; \tag{2.72}$$

means that the first term on the right-hand side vanishes and that we can write the Euclidean action as

$$S_{\mathrm{T}}^{\mathrm{E}} = \int_0^{} \mathrm{d} \int_0^{} \mathrm{d}x \, \frac{1}{2} Q \left[l@^2 - \frac{1}{c}@_x^2 \right] Q = \int_0^{} \mathrm{d} \int_0^{} \mathrm{d}x \, \frac{1}{2} QAQ; \tag{2.73}$$

where we have defined $A \quad l@^2 - \frac{1}{c}@_x^2$.

Now, we want to compute the effective action we get by coupling our Josephson chain to two transmission lines, one on either side. Our calculations for this will be inspired by those in [26, 27]. Let us first consider the transmission line to the right of the Josephson chain. An identical calculation can be done for the left

[P] $@_x Q(x; \ )j_{x=0} = 0$ h09j §\9§§\0H\9}X0nj §\0 0jL nT§\0H\9_j _ 0x«9e§n§\0H\9}X0nj §\0 0jL nT§\0§}9j h_ _nj e_j0u $@_x Q(x; \ )j_{x=1} = 0$ _jH0 $c^{\,1}@_x Q(x; \ )j_{x=1} = V(x; \ )j_{x=1} = 0$u

transmission line. By performing a mean over all configurations which holds the charge on the right end of the chain fixed to $Q_{L_x}(\ )$, we can compute an effective action $S_{L_x J 0}$, as

$$e^{\ S_{L_x J 0}} = \int D[Q] e^{\ (S + S_T^E)}\ [Q(0;\ ) \quad Q_{L_x}(\ )]; \tag{2.74}$$

where S is the action for the Josephson chain (2.63). Now, let us make the definition $S_{L_x J 0} \quad S + S_{L_x J\_j §}$. To find $S_{L_x J 0}$ we only need to find the interaction action $S_{L_x J\_j §}$. We find that

$$\begin{aligned} e^{\ S_{L_x J\_j §}} &= \int D[Q] e^{\ S_T^E[Q]}\ [Q(0;\ ) \quad Q_{L_x}(\ )] \\ &= \int D[Q] \int D[\ '] e^{\ \int d \int dx \frac{1}{2} QAQ + i \int_0 d\ \ '(\ )(Q(0;\ ) \quad Q_{L_x}(\ ))} \\ &= \int D[Q] \int_1^1 D[\ '] e^{\ \int d \int dx \frac{1}{2} QAQ + i \int_0 d \int dx\ '(\ )Q(x;\ )\ (x)} \\ &\qquad e^{\ i \int d\ \ '(\ )Q_{L_x}(\ )}; \end{aligned} \tag{2.75}$$

where we expanded the delta functional in a Fourier series. Now, use the result for Gaussian integrals $\int D[\ '] e^{\ \int d^n x[\ \frac{1}{2}\ ' A\ ' + iJ\ ']} \ / \ e^{\ \frac{1}{2} \int d^n x \int d^n y\ J(x) A^{\ 1}(x;y) J(y)}$ where $AA^{\ 1}(x;y) = \ (x \quad y)$. This yields:

$$\begin{aligned} e^{\ S_{L_x J\_j §}} &= C \int_1^1 D[\ '] e^{\ \frac{1}{2} \int d \int dx\ '(\ )\ (x) \int dx^0 d\ ^0 A^{\ 1}(x;\ ;x^0;\ ^0)\ '(\ ^0)\ (x^0)} \\ &\qquad e^{\ i \int d\ \ '(\ )Q_{L_x}(\ )} \\ &= C \int_1^1 D[\ '] e^{\ \frac{1}{2} \int d\ \ '(\ ) \int d\ ^0 A^{\ 1}(0;\ ;0;\ ^0)\ '(\ ^0) \ i \int d\ \ '(\ )Q_{L_x}(\ )} \\ &= C^0 e^{\ \frac{1}{2} \int d\ d\ ^0 Q_{L_x}(\ )M(\ ;\ ^0)Q_{L_x}(\ ^0)}; \end{aligned} \tag{2.76}$$

where $M(\ ;\ ^0) \quad (A^{\ 1}(0;\ ;0;\ ^0))^{\ 1}$ and $C; C^0$ are some irrelevant constants. Now, expanding $(x \quad x^0)\ (\ \ ^0)$ in a Fourier series and using that

$$A^{\ 1}(x;\ ;x^0;\ ^0) = \frac{1}{2} \sum_{!_n} \int e^{i[kx \quad !_n\ ]} A^{\ 1}(k; !_n; x^0;\ )\ dk; \tag{2.77}$$

we find that

$$A^{\ 1}(k; !_n; x^0;\ ^0) = \frac{e^{\ i[kx^0 \quad !_n\ ^0]}}{l !_n^2 + \frac{k^2}{c}}; \tag{2.78}$$

where $!_n = \frac{2\ n}{}$ and $n = 0;\ \ 1;\ \ 2; : : :$ An inverse Fourier transformation then yields

$$A^{\ 1}(x;\ ;x^0;\ ^0) = \frac{1}{2} \sum_{!_n} \int dk\ \frac{e^{i[k(x \quad x^0) \quad !_n(\ \ ^0)]}}{l !_n^2 + \frac{k^2}{c}}: \tag{2.79}$$

Now, we can to compute $M^{-1}(\ ;\ ^0) = A^{-1}(0;\ ;0;\ ^0)$. We get that

$$M^{-1}(\ ;\ ^0) = \frac{1}{2}\sum_{!_n} \int dk\, \frac{e^{\,i!_n(\quad ^0)}}{l!\frac{2}{n} + \frac{k^2}{c}} = \frac{1}{2}\sqrt{\frac{c}{l}}\sum_{!_n}\frac{1}{j!_n j} e^{\,i!_n(\quad ^0)}; \tag{2.80}$$

and by Fourier transforming and inverting we find the inverse as

$$M(\ ;\ ^0) = \frac{2}{}\sqrt{\frac{l}{c}}\sum_{!_n} j!_n j e^{\,i!_n(\quad ^0)}: \tag{2.81}$$

Now, for a semi-infinite transmission line we have that the real impedance R is equal to $\sqrt{l=c}$ [13]. Inserting this expression for $M(\ ;\ ^0)$ into the expression for $e^{\,S_{L_x}J_{-}j\S}$ yields:

$$\begin{aligned} e^{\,S_{L_x}J_{-}j\S} &/ e^{\,\frac{1}{2}\int d\ d\ ^0 Q_{L_x}(\ )M(\ ;\ ^0)Q_{L_x}(\ ^0)} \\ &= e^{\,\frac{1}{2}\sum_{!_n} 2j!_n j\int d\ e^{\,i!_n\ Q_{L_x}(\ )}\int d\ ^0 e^{i!_n\ ^0}Q_{L_x}(\ ^0)} \\ &= e^{\,\frac{1}{2}\sum_{!_n} 2Rj!_n jjQ_{L_x}(!_n)j^2}; \end{aligned} \tag{2.82}$$

where $Q_{L_x}(!_n) = \int d\ e^{\,i!_n}\ Q_{L_x}(\ )$. Now, introducing the dimensionless charge $q_{L_x}(\ ) = \frac{Q_{L_x}(\ )}{2e}$ and the quantum resistance $R_Q = \frac{h}{(2e)^2}$, this can be simplified to:

$$e^{\,S_{L_x}J_{-}j\S} / e^{\sum_{!_n}\frac{2\ Rj!_n j}{R_Q}jq_{L_x}(!_n)j^2} = e^{\sum_{!_n}\frac{2\ R}{R_Q\ j!_n j}jJ^x_{L_x}(!_n)j^2}; \tag{2.83}$$

where $J^x_{L_x}(\ ) = \frac{@q_{L_x}}{@}$) $J^x_{L_x}(!_n) = \quad i!_n q_{L_x}(!_n)$. The divergence for $!_n = 0$ can be ignored due to the periodic boundary conditions of $q_{L_x}(\ )$:

$$J^x_{L_x}(!_n = 0) = \int_0 d\ J^x_{L_x}(\ ) = \int_0 d\ @\ q_{L_x}(\ ) = q_{L_x}(\ ) \quad q_{L_x}(0) = 0: \tag{2.84}$$

So far in this section we have assumed that is continuous. However, we discretized time in section 2.4.2. For the two parts to fit together we must discretize equation (2.83). From the discretization of the Fourier transform, we get that

$$jJ^x_{L_x}(!_n)j^2 = \Big|\sum_{=0}^{L-1} e^{i!_n}\ J^x_{L_x}(\ )\Big|^2 = \sum_{;\ ^0=0}^{L-1} e^{i!(\quad ^0)}J^x_{L_x}(\ )J^x_{L_x}(\ ^0): \tag{2.85}$$

The factor $j!_n j$ in (2.83) comes from the Fourier transform of the derivative $@\ q_{L_x}$. In the discretized case this will change. Using the definition (2.57) of $q_{L_x;}$ and Fourier transforming, we get that:

$$J^x_{L_x}(\ ) = \sqrt{r}\ q_{L_x;} = \frac{q_{L_x;} \quad q_{L_x;\ -1}}{} \ F\ !\ J^x_{L_x}(!_n) = \frac{2\sin\ \frac{!_n}{2}\ e^{\frac{i!_n}{2}}}{}q_{L_x}(!_n): \tag{2.86}$$

So in (2.83) we should replace $jq_{L_x}(!_n)j^2$ with $j\frac{}{2\sin(\frac{!_n}{2})}j^2 jJ^x_{L_x}(!_n)j^2$ and $j!_n j$ with $j\frac{2}{}\sin\frac{!_n}{2}j$. We can note that $j\frac{2}{}\sin\frac{!_n}{2}j\ !\ j!_n j$ as $\quad !\ 0$.

This means that we get our final expression

$$S_{L_x\mathrm{J\_j\S}} = \frac{2\ R}{R_Q}\sum_{n=1}^{L\mathrm{X}\ 1}\frac{jJ^x_{L_x}(\ !_n)j^2}{j\frac{2}{2}\sin\frac{!_n}{2}j} = \frac{2\ R}{R_Q L}\sum_{;\ ^0=0}^{L\mathrm{X}\ 1} J^x_{L_x}(\ \ )J^x_{L_x}(\ \ ^0)B_{\ ;\ ^0}; \qquad (2.87)$$

where we have defined

$$B_{\ ;\ ^0} \sum_{n=1}^{L\mathrm{X}\ 1}\frac{e^{i\,!_n\ \ (\ \ \ ^0)}}{j2\sin\frac{!_n}{2}j}: \qquad (2.88)$$

Of course, one gets an analogous expression if one considers the interaction from the left transmission line $S_{0\mathrm{J\_j\S}}$;

$$S_{0\mathrm{J\_j\S}} = \frac{2\ R}{R_Q L}\sum_{;\ ^0=0}^{L\mathrm{X}\ 1} J^x_0(\ \ )J^x_0(\ \ ^0)B_{\ ;\ ^0}: \qquad (2.89)$$

The total action S_{tot} for the system, including the influences of the transmission lines, is therefore given by $S_{\mathrm{tot}} = S + S_{0\mathrm{J\_j\S}} + S_{L_x\mathrm{J\_j\S}}$, where S is given by (2.63). Note that from section 2.3 corresponds to $R_Q=(2R)$ in our system, with an emphasis on the two, since there are two transmission lines.

From (2.89), one can in fact get a hint of the Schmid(-Bulgadaev) transition using the following somewhat hand-waving argument: imagine a system for a single Josephson junction where the two ends of the transmission lines are connected, such that $J^x_0(\ \ ) \quad J^x_{L_x}(\ \ )$. The dissipative term in the total action is then given by $S_{\mathrm{dis}} = 2S_{0;\mathrm{int}}$. For simplicity, the other parts of the action are not considered in this argument. The energy cost S_{dis} of adding a link in an otherwise empty system, i.e. $J^x_0(\ \ ) = 0$ for all , is given by $\frac{4}{R_Q}\frac{R}{L}B_{\ ;\ }$. In the continuous limit $L \ ! \ 1$, and with $= \ ^0$, we see that (2.88) is replaced by

$$B_{\ ;\ } = \sum_{n=1}^{L\mathrm{X}\ 1}\frac{1}{j\quad !_n j} = \frac{L}{2}\sum_{n=1}^{L\mathrm{X}\ 1}\frac{1}{n} \ ! \ \frac{L}{2}\log L\ : \qquad (2.90)$$

Hence $S_{\mathrm{dis}} = \frac{2R}{R_Q}\log L$. The system can qualitatively be described by two competing forces: the entropy gain and the energy cost from the addition of a link-current. The entropy gain of placing a link-current in the system with uniform probability is $\log L$. A phase transition should take place when the energy cost of adding a link-current equals the entropy gain:

$$\frac{2R}{R_Q}\quad 1\ \log L\ = 0: \qquad (2.91)$$

We see that the two forces match for $2R=R_Q = 1$. This reasoning confirms the idea of the Schmid(-Bulgadaev) transition.

©u£ w«9j§«h q\9 0 e_q 9jL 9 x«9j§«h q\9 0 §}9j _§_nj

In section 2.4 we mentioned that the Hamiltonian for a Josephson chain consists of two terms, and that the strength ratio of these is given by the superconducting stiffness K. We argued that the chain should be in a superconducting state if K 1 and an insulating state if K 1. The natural next step is to investigate the system for intermediate values of K.

To analyze this, one should know that an infinite d-dimensional Josephson junction array is at zero temperature and for 1 in the same universality class as the classical $d + 1$-dimensional XY-model, which, for $d + 1 = 2$, is known to exhibit a Berezinskii-Kosterlitz-Thouless (BKT) phase-transition at a critical temperature T_c [4]. Josephson junction arrays therefore also show BKT-transitions but with the critical temperature replaced with a critical value of K.

A BKT-transition involves the binding and unbinding of topological vortices with logarithmic interactions. For Josephson arrays the topological excitations are quantum phase slips, which corresponds to vortices in space-time [4]. It is possible to map the XY-model onto a 2-dimensional Coulomb gas, where these vortices are seen as "charges". In the superconducting phase the vortices will be ordered in vortex-antivortex configurations (dipoles). When K is decreased below the critical value K_c, the vortices will un-bind and transition into a plasma phase. This is the insulating phase.

The two phases can be understood from the Josephson relation (2.9). According to this, one expects that a phase slip leads to a voltage drop. In the superconducting phase where the phase slips are bound into pairs with opposite signs, one does not measure a voltage drop over a macroscopic region. In the insulating regime, the phase-slips are not paired, and any current will lead to a voltage.

The mapping of phase slips onto an interacting gas was first made by Bradley and Doniach [5]. They considered the case with only self-capacitance i.e. $C = 0$. They found that the critical value of $\sqrt{E_J/E_{C_0}}$ for an infinite chain was 0:79. Above this value, the phase correlator will decay algebraically and so we get a quasi-long-range order of the phase. The chain is in a superconducting state. Below this value, the chain is in an insulating state.

The results of Bradley and Doniach was later extended by Choi et al. [7] and Korshunov [6] to finite values of C (see also [22]). They found that in the limit ! 1, the critical value is $\sqrt{E_J/E_{C_0}} = 2/$ and constructed the schematic phase diagram displayed in figure 2.4a.

In experiments, where we have a finite chain and a dissipative environment, the phase diagram becomes more complicated. In an attempt to explain the results of experiments on short nanowires (which can be modeled as a finite Josephson junction chain), Büchler et al. considered the influence of the leads connected to the ends of the wire [28] (see also [29]). In their study, an impedance with static resistance R_p coupled parallel to the wire defined the environment. Their main result

could be summarized as a schematic phase diagram for the wire, see figure 2.4b, where is the dimensionless admittance characterizing the wire's superconducting properties. The quantity corresponding to in Josephson chains is $\sqrt{E_J/E_{C_0}}$. As shown in the diagram, they found that the Schmid transition discussed in section 2.3 determines whether the wire is in a superconducting or insulating state. They also found that the phase transition for an infinite wire (corresponding to the Josephson chain transition at $\sqrt{E_J/E_{C_0}} = 2/\pi$) survived in the superconducting phase, but that it turned into a H}n n®0}. However, this crossover is only relevant if the temperature is sufficiently high. The conclusion of this study is that large dissipation, meaning a small value of R_p/R_Q, protects the superconducting state in the short nanowire, and that states, that in the case of no dissipation would be insulating (i.e. states where < 2), become superconducting, although weakly.

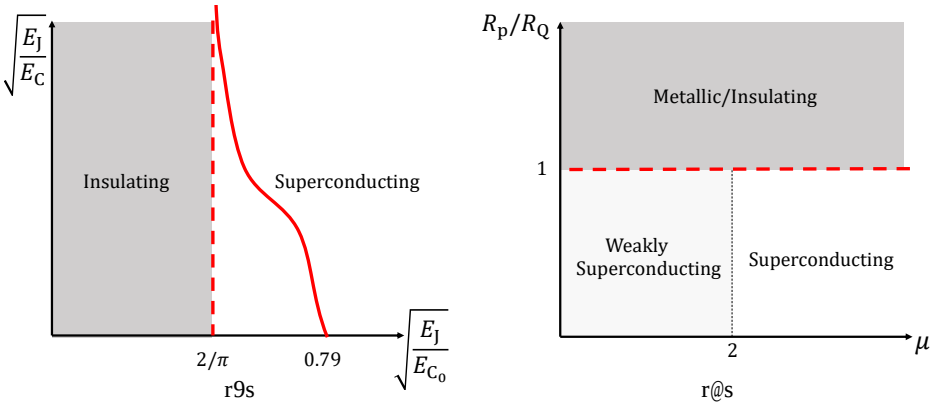

Figure 2.4: a) The schematic phase diagram for an infinite Josephson junction chain without any dissipation and $T = 0$. b) The schematic phase diagram found by Büchler et al. for a finite superconducting nanowire.

©u¢ Sn} h «e9§_n j _j §0} h nT ¼« ² x«9 j §9

In this section we will use an alternative way to describe the Josephson chain (we will follow [23, 24]); instead of considering each individual superconducting island, we will regard the whole system as a single lumped circuit element. Instead of the charges and phases on the superconducting islands as the degrees of freedom, we will consider the number of magnetic flux quanta crossing the chain. The Josephson chain in terms of the number of flux quanta n can be formulated as a tight-binding Hamiltonian:

$$\hat{H} = \sum_n E_0 |n\rangle\langle n| - \sum_{n;m} t_m (|n+m\rangle\langle n| + |n\rangle\langle n+m|); \qquad (2.92)$$

where E_0 is the ground state energy without tunneling and t_m is the transition amplitude for the simultaneous tunneling of m flux quanta (as the tunneling of a flux quantum is associated with a quantum phase slip event, t_m is the phase slip amplitude). In the superconducting phase, the t_m where $m = 1$ will be dominating. The eigenstates $|k\rangle$ and the corresponding eigenvalue E_k can be found by realizing that the Hamiltonian is translation invariant in n:

$$|k\rangle = \frac{1}{\sqrt{N}} \sum_n e^{ikn} |n\rangle; \quad E_k = E_0 \sum_{m=1}^{N} 2t_m \cos(km); \quad 0 \quad k < 2 \; ; \tag{2.93}$$

where, for normalization purposes, we have limited the number of phase slips to N. We will eventually let $N \; ! \; 1$. Our goal is to relate these quantities to those that are simulated using (2.63).

Consider now the partition function Z_m restricted to configurations where the net vorticity is exactly m. Quantum mechanically this corresponds to a matrix element

$$Z_m = \langle n + m | e^{-\hat{H}} | n \rangle : \tag{2.94}$$

Due to the n-symmetry in $\hat{H}$, Z_m does not depend on n. Z_m can be interpreted as the transition amplitude for the system to be in a state $|n\rangle$ at imaginary time $= 0$ and evolve in imaginary time to end up in state $|n + m\rangle$ at $=$. Let us now consider

$$\begin{aligned} e^{-E_k} &= \langle k | e^{-\hat{H}} | k \rangle = \frac{1}{N} \sum_{n;n^0} \langle n^0 | e^{-\hat{H}} | n \rangle e^{ik(n - n^0)} \\ &= \frac{1}{N} \sum_{n;m} \langle n + m | e^{-\hat{H}} | n \rangle e^{ikm} = \sum_m Z_m e^{ikm}; \end{aligned} \tag{2.95}$$

where we did the substitution of variables $m = n - n^0$. Defining $E_k - E_k - E_0$, we get that (in the limit $! \; 1$ [24])

$$e^{-(E_k - E_0)} = e^{-E_k} = \frac{\langle k | e^{-\hat{H}} | k \rangle}{\langle 0 | e^{-\hat{H}} | 0 \rangle} = \frac{\sum_m Z_m e^{ikm}}{\sum_m Z_m} = e^{ikm} \; : \tag{2.96}$$

Let us now return to (2.63). We discussed at the end of section 2.4.2 that the partition function could be expressed as a sum over the integer field v_x, which represented vortices. For convenience, we will restate it here:

$$Z = \sum_{\{q_x\}} e^{-(S_J + S_Q[q])} = \sum_{\{v_x\}} \int Dq_x \, e^{-(S_J + S_Q[q]) \; 2 \; i \sum_x q_x \; v_x} : \tag{2.97}$$

Since each vortex correspond to a flux quantum, we can identify $m = \sum_{x;} v_{x;}$, where we let $N \to 1$. We can now express e^{ikm} as

$$e^{ikm} = e^{ik \sum_{x;} v_{x;}} = \frac{\sum_{fv_x g} \int Dfq_{x;} g e^{(S_J + S_Q) \, 2i \sum_x (q_x - \frac{k}{2}) v_x}}{\sum_{fv_x g} \int Dfq_{x;} g e^{(S_J + S_Q) \, 2i \sum_x q_x v_x}}$$
$$= \frac{\sum_{fq_x g} e^{(S_J + S_Q[q - \frac{k}{2}])}}{\sum_{fq_x g} e^{(S_J + S_Q[q])}} = \frac{\sum_{fq_x g} e^{(S_J + S_Q[q])} e^{-S_k}}{\sum_{fq_x g} e^{(S_J + S_Q[q])}} = e^{-S_k}; \tag{2.98}$$

where we have defined $S_k \equiv S_Q[q - \frac{k}{2}] - S_Q[q]$. From (2.63) this can be computed as

$$S_k = \frac{E_C}{2} \sum \Big(\Big[\sum_j q_{j;} - \frac{k}{2} \Big]^2 \sum_i n_i \, G_{i;L_x} - G_{i;1} \Big]^2 - \Big[\sum_j q_{j;} \Big]^2 \sum_i n_i \, G_{i;L_x} - G_{i;1} \Big]^2 \Big)$$
$$= \frac{E_C}{2} \sum \Big[\frac{k^2 (L_x - 1)^2}{4} - \frac{2k(L_x - 1)}{2} Q \Big]; \tag{2.99}$$

where E_C is given by (2.62) and Q is given by (2.61). From (2.96) and (2.98) we see that we can compute E_k as

$$E_k = -\frac{1}{\beta} \log \langle e^{-S_k} \rangle = -\frac{1}{\beta} \log \frac{Z_k}{Z}; \tag{2.100}$$

where

$$Z_k = \sum_{fq_{x;} g} e^{(S_J + S_Q[q] - S_k)}. \tag{2.101}$$

We have now related E_k from (2.93) to the quantities in (2.63). Let us now interpret the physical meaning of E_k and k. From e.g. (2.98) we see that k represent, up to factor of $2e=2$, exactly an externally imposed displacement of the charge field $q_{x;}$. E_k then gives the energy dependence of the ground state on this charge displacement. We can thus compute an effective inverse capacitance C_k^{-1} defined as

$$C_k^{-1} \equiv \frac{2}{2e}^2 \frac{\partial^2 E_k}{\partial k^2} \tag{2.102}$$

as an effective response function due to this charge displacement. Using equations (2.100) and (2.99), this can be calculated as

$$\begin{aligned} C_k^{-1} &= \frac{2}{2e}\,{}^2\!\left[-\frac{\partial^2 E_k}{\partial k^2}\right] \\ &= \frac{2}{2e}\,{}^2\!\left[-\left\langle\frac{\partial^2 S_k}{\partial k^2}\right\rangle + \left\langle\frac{\partial S_k}{\partial k}\right\rangle^2 + \left\langle\frac{\partial S_k}{\partial k}\right\rangle^2\right] \\ &= \frac{E_C(L_x-1)^2}{(2e)^2}\left[1 - \frac{E_C}{L}\left\langle Q^2\right\rangle_k + \left\langle Q\right\rangle_k^2\right]; \end{aligned} \tag{2.103}$$

where we defined $Q \equiv \sum_P Q$. C_k^{-1} with $k = 0$, for which $\langle Q\rangle_k = 0$, will be used in the simulations as a measure of the degree of superconductivity of the Josephson junction chain. In the superconducting state we should have no voltage across the Josephson chain and in this regime $C_{k=0}^{-1} \to 0$. Deep in the insulating state, the charge fluctuations are suppressed and so $C_{k=0}^{-1} \to \frac{E_C(L_x-1)^2}{(2e)^2}$. For a single Josephson junction (i.e. $L_x = 2$), this limit can be simplified to $C_{k=0}^{-1} = C^{-1} + 2C_0^{-1}$, which is the total inverse capacitance for a system with three capacitors with capacitances C, C_0 and C_0 coupled in series.

In the Monte Carlo simulations described in chapter 3 we will not compute the actual inverse capacitance $C_{k=0}^{-1}$ but instead a normalized inverse capacitance $\tilde{C}_{k=0}^{-1} = \frac{(2e)^2}{E_C(L_x-1)} C_{k=0}^{-1}$. We have that in the superconducting regime $\tilde{C}_{k=0}^{-1} \to 0$ and in the insulating regime $\tilde{C}_{k=0}^{-1} \to L_x - 1$.

G\9q§0} ¨

¦ \0 g nj§0 G9}en h0§\nL

In equilibrium statistical physics, one is frequently interested in a quantity which involves the evaluation of a sum or integration over the state space of a system, such as (2.63). Most often, the state space of the system is so large that is practically impossible to perform the integration even on a computer. The key principle behind Monte Carlo simulations is to replace this summation with a summation over a subset of randomly, but carefully, chosen states, from which the desired quantity can be estimated.

In this chapter, we will in section 3.1 briefly go through some basic principles of Monte Carlo simulations. More detailed accounts can be found in e.g. [30–33]. In section 3.2 we go on describing the Monte Carlo method employed in this thesis in detail. In section 3.3 we discuss the different parameters we will investigate and how to choose them. The final section 3.4 gives an overview of the algorithm, and a few comments on the code implementation.

¨uo ~n h0 @9 _H nT g nj§0 G9}en _h «e9§_nj

Let us consider a system which can be in a set of states $f_i g$ and let p_i be the probability for the system to be in state i. Then the average of a quantity Q is given by

$$hQi = \sum_i Q_i p_i; \tag{3.1}$$

where Q_i is the value of Q when the system is in state $_i$. Usually one is interested in the canonical ensemble where we have the Boltzmann distribution:

$$p_i = \frac{e^{E_i}}{Z}; \quad Z = \sum_i e^{E_i}; \tag{3.2}$$

where E_i is the energy of the system in state i. Inserting this into to (3.1) yields:

$$\langle Q \rangle = \sum_i Q_i p_i = \frac{1}{Z} \sum_i Q_i e^{-E_i} : \tag{3.3}$$

In Monte Carlo simulations we generate a subset of states $\{1; : : : ; M\}$ from which we estimate $\langle Q \rangle$. Say that these states are chosen with uniform probability. Then the estimate is given by:

$$\langle Q \rangle \quad Q_M = \frac{\frac{1}{M} \sum_{i=1}^{M} Q_i e^{-E_i}}{\frac{1}{M} \sum_{i=1}^{M} e^{-E_i}}; \tag{3.4}$$

where Q_M is called the 0 §_h9§n} and $Q_M \to \langle Q \rangle$ when $M \to 1$. However, to choose all states with an equal probability is very inefficient since most of the states are very improbable and will not contribute much to the thermodynamic average. Instead, we use the technique called _hqn}§9jH0 9hqe_jX to generate states according to some distribution p'. We will write this as $i \; 2 \; p'$. The Monte Carlo estimate of $\langle Q \rangle$ is then given by:

$$Q_M = \frac{\sum_{i=1}^{M} Q_i e^{-E_i}}{\sum_{j=1}^{M} e^{-E_j}} = \frac{\sum_{i=1}^{M} Q_i p'^{-1}_i e^{-E_i} p'_i}{\sum_{j=1}^{M} p'^{-1}_j e^{-E_j} p'_j} = \frac{\sum_{i \; 2 p'; i=1}^{M} Q_i p'^{-1}_i e^{-E_i}}{\sum_{j \; 2 p'; j=1}^{M} p'^{-1}_j e^{-E_j}} : \tag{3.5}$$

We must now choose which probability distribution p' to use. One suggestive way to choose it, which also often is efficient enough, is to pick the Boltzmann distribution $p' = Z^{-1} e^{-E}$. The equation for the estimator then becomes a simple arithmetic average

$$Q_M = \frac{1}{M} \sum_{i \; 2 p'; i=1}^{M} Q_i : \tag{3.6}$$

The natural question that now arises is how one picks out states so that they appear according to the Boltzmann distribution. The standard solution is to utilize a Markov process.

¨uouo g 9}cn® q}nH0

For our purposes, a Markov process is a mechanism which generates a new state from an old state in a random fashion. The probability of generating the new state is given by the §}9j _§_nj q}n@9@_e_§´ $P(\quad \to \quad)$. In a Markov process, the transition probability should not depend on time and only depend on the states

and and not on the previous history of states, i.e. it "has no memory". We naturally also have the normalization condition

$$\sum_{} P(\quad ! \quad) = 1: \tag{3.7}$$

The Markov process is repeatedly used to generate a g9}cn® H\9_j of states. Starting with a state $_1$, we use that to generate a new state $_2$, which is fed into the process to yield a state $_3$ and so on. When run long enough, the Markov process is chosen specially so that it produces our chosen Boltzmann distribution p^0 . To achieve this, two additional conditions is set on the Markov process, namely that of 0}XnL_H_§´ and LO§9_e0L @9e9jH0.

¨uou© N}XnL_H_§´ 9jL LO§9_e0L @9e9jH0

The condition of ergodicity simply says that the Markov process should be able to reach any state from any state , if it is repeated enough times. Since every state appear with some non-zero probability, this is simply required if we are to generate states with the correct Boltzmann distribution.

The requirement of detailed balance can be showed to be sufficient (although not necessary) to ensure that the distribution we generate when the system has reached equilibrium is indeed our chosen Boltzmann distribution, and no other distribution [30]. The condition for detailed balance can be formulated as:

$$p \; P(\quad ! \quad) = p \; P(\quad ! \quad): \tag{3.8}$$

Inserting the Boltzmann distribution, this can be simplified as:

$$\frac{P(\quad ! \quad)}{P(\quad ! \quad)} = e^{\quad (E \quad E \;)}: \tag{3.9}$$

Equations (3.7) and (3.9) are the constraints on our choice of the transition amplitude. If these are satisfied, together with the ergodicity condition, then the Boltzmann distribution will be the equilibrium distribution in our Markov process.

¨uou¨ 8HH0q§9jH0 }9§_n

A convenient way to write the transition amplitude is to divide it into two parts: $P(\quad ! \quad) = s(\quad ! \quad)A(\quad ! \quad)$, where $s(\quad ! \quad)$ is the 0e0H§_nj q}n@9@_e_§´ (also called proposal probability), and $A(\quad ! \quad)$ is the 9HH0q§9jH0 }9§_n. The condition for detailed balance is then written as:

$$\frac{P(\quad ! \quad)}{P(\quad ! \quad)} = \frac{s(\quad ! \quad)A(\quad ! \quad)}{s(\quad ! \quad)A(\quad ! \quad)} = e^{\quad (E \quad E \;)}: \tag{3.10}$$

Given that $s(\quad ! \quad)$ is fixed by the specific algorithm we choose to employ, we still have the freedom to choose the acceptance ratio so long it as it is between

0 and 1 and fulfills detailed balance. However, for efficiency we want to choose the acceptance ratios to be as large as possible. This leads to using the choice of Metropolis-Hasting:

$$A(\quad ! \quad) = \min \quad 1; \frac{s(\quad ! \quad)}{s(\quad ! \quad)} e^{\quad (E \quad E \quad)} = \min \quad 1; \frac{s(\quad ! \quad)}{s(\quad ! \quad)} e^{\quad S(\quad ! \quad)}; \tag{3.11}$$

where we in the second equality returned to the notation of chapter 2.

¨uouV N}}n} 0 §_h9§_nj

Due to the statistical nature of Monte Carlo computations, errors in a computed quantity Q are unavoidable. To determine whether the result obtained from a Monte Carlo simulation is any good, one needs to make an estimate of the magnitude of the error. There are many ways to do this, however in this thesis we will use a very simple and general method called the blocking method [30]. The idea is to divide the computations of the quantity Q into N_b blocks. An average estimate is then computed separately in each block. The error can then be estimated by the standard deviation:

$$= \sqrt{\frac{1}{N_b \quad 1} \sum_{i=1}^{N_b} (hQ_i^2 i \quad hQ i_b^2)}; \tag{3.12}$$

where Q_i is the average over block i and hQi_b the average over all blocks. Important to note is that this estimate is accurate only if each block is large enough such that the block averages are uncorrelated.

This method is simple and works for almost any quantity Q, even though it is not completely rigorous since the number of blocks will clearly affect the calculation of the standard deviation. Still, it will give a reasonable estimate on the order of magnitude of the error and it is good enough for our purposes.

¨u© ¯n}h 9eXn}_§\h

In the model (2.63), the degrees of freedom are integer-valued, divergence-free link-currents $J_{x;} = (J^x_{x;}; J_{x;}) \; 2 \; Z^2$ (which sometimes are called J-currents or bond-currents). The $q_{x;}$ -variables in (2.63) have a linear relation with the link-currents.

Physically, $J^x_{x;}$ represent the current between island x and $x + 1$ at imaginary time and $J_{x;}$ is the number of Cooper pair on island x during time-slice . The constraint of current conservation implies that the link-currents form closed loops. In our simulations we will generate these loops via a so called °n}h 9eXn}_§\h.

These divergence-free link-currents can namely graphically be represented as worms on a lattice with periodic boundary conditions in the time direction, see figure 3.1. The height of the lattice is L = and the width is $L_x + 2$. The superconducting islands are the black dots with x-coordinates from $x = 1$ to $x = L_x$.

The white dots represent the transmission lines. These should be regarded as "helper points", allowing the worm to leave the Josephson chain at a time , and to rejoin it at a time ^{0}.

As discussed in chapter 2.4.2, the $q_{x;}$ -variables can be regarded as a height field living on the lattice. The link-currents enclose areas where the value of the field is constant. It is negative if the worm is circulating in a clockwise direction, and positive if it is circulating in an anti-clockwise direction. Naturally, just as the $J^{x}_{x;}$ - and $J_{x;}$ -variables, the $q_{x;}$ -variables can take any integer value.

To describe the worm algorithm, let us first introduce some notation. Let us denote each lattice site as $\mathbf{s} = (x; \ )$ with link-currents $J_{x;}$ between them, where $= x; \ $. We will use the notation where $J^{x}_{x;}$ extends between $(x; \ )$ and $(x + 1; \ )$ and $J_{x;}$ extends between $(x; \ )$ and $(x; \ + 1)$. We will update the values of these link-currents using a worm whose "head" is visiting a set of points $f\mathbf{s}_i g$ where $\mathbf{s}_i = (x_i; \ _i)$. Lastly, let us denote the distance between the head and the tail of the worm in the -direction as W . This is needed since we are simulating a canonical ensemble for which $W = 0$ must be satisfied. The worm algorithm can now be described as follows:

1. Choose a random starting site $\mathbf{s}_0 = (x_0; \ _0)$ in the lattice.

2. Choose a direction $= x;$ out of the possible directions with uniform probability. The change acceptance rate A_{s_i} for adding a link in that direction is computed.

3. With probability A_{s_i}, move the head of worm from the site $\mathbf{s}_i$ to the new site $\mathbf{s}_{i+1}$. With probability $1 \quad A_{s_i}$, go to 2.

4. Update the correct link-current $J^{j \ j}_{x_i; \ _i}$. If the head of the worm leaved the site $\mathbf{s}_i$ by going the in a positive x- or -direction, the corresponding link-current $J^{j \ j}_{x_i; \ _i}$ is _jH}0h0j§0L by 1: $J^{j \ j}_{x_i; \ _i} \ ! \ J^{j \ j}_{x_i; \ _i} + 1$. If the head of the worm leaved the site $\mathbf{s}_i$ by going the in a negative direction, the corresponding link-current $J^{j \ j}_{x_i \quad x;j \ j; \ i \quad ;j \ j}$ is L0H}0h0j§0L by 1: $J^{j \ j}_{x_i \quad x;j \ j; \ i \quad ;j \ j} \ ! \ J^{j \ j}_{x_i \quad x;j \ j; \ i \quad ;j \ j} \ 1$. Also, update Q (see section 3.2.1).

5. Repeat step 2-4 until $\mathbf{s}_i = \mathbf{s}_0$ and $W = 0$.

6. At this point, the worm is closed. Collect statistics for the relevant quantities which can be computed with MC estimators. Then go to 1 and repeat until the estimate converge.

This algorithm clearly fulfills ergodicity. The question is now how to compute the acceptance ratios A_{s_i} for all lattice positions s_i and directions such that detailed balance is fulfilled.

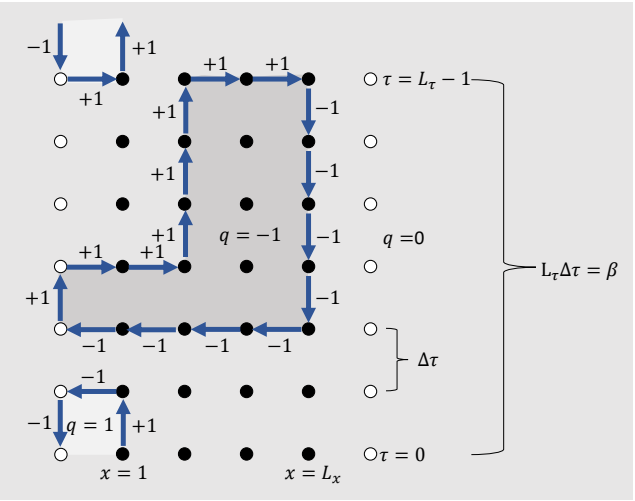

Figure 3.1: An illustration of the space-time lattice with two completed worms. The numbers next to the arrows represent the values of $J_{x;\ }$.

¨u©uo S_jL_jX §\0 9HHOq§9jHO }9§_n

We will use the Metropolis-Hastings choice (3.11) for our acceptance ratios. We see that these are largely dependent on the change in the action $S(\ \ !\ \ )$. This will be computed from (2.63) if the worm is moving in the chain (x 2 $[1; L_x]$), and (2.87) and (2.89) if the worm is entering or leaving one of the transmission lines. Special care must be taken when the worm is in either of the transmission lines and is moving in the -direction (see below). The following sections will be dedicated to calculating the values of $S(\ \ !\ \ )$.

However, when the worm is leaving or joining the Josephson chain, we must also consider the selection probabilities. When the head of the worm is on the edge ($x = 0$ or $x = L_x + 1$), it cannot move outside the lattice so the selection probability that it attempts to move in the lattice is 1=3. The selection probability that it attempts to move out to the transmission line when it is on the edge of the Josephson chain is 1=4. Let $_{x=1=L_x}$ and $_{x=0=L_x+1}$ denote states in which the worm head is on the edge of the Josephson chain and outside the Josephson chain, respectively. Then $s(\ _{x=1=L_x}\ !\ _{x=0=L_x+1}) = 1=4$ and $s(\ _{x=0=L_x+1}\ !\ _{x=1=L_x}) = 1=3$. Therefore, we get the acceptance ratios:

$$\begin{aligned} A(\ _{x=1=L_x}\ !\ _{x=0=L_x+1}) &= \min\ 1; \frac{4}{3}e^{\ \ S_T}\ ; \\ A(\ _{x=0=L_x+1}\ !\ _{x=1=L_x}) &= \min\ 1; \frac{3}{4}e^{\ \ S_T}\ : \end{aligned} \tag{3.13}$$

Now, let us first consider the case where the worm moves in the Josephson chain and then when it enters and leaves it.

g n®_jX §\O °n}h _j §\O `n Oq\ nj H\9_j

In the action (2.63) we see that S_J depends only on the link-variables $J_{x;}$ and S_Q on the $q_{x;}$ - and $J_{x;}$ -variables. Let us first consider the change in the action S_J when we add a link-current in the -direction at position $(x;t)$ where $= x;$. We have that $S_J = S_J[J_{x;t} \quad _{x;t}] \quad S_J[J_{x;t}]$. After some simplifications, we find that

$$S_J{}^x = \log \frac{I_1(E_J \quad)}{I_0(E_J \quad)} (\quad 2J^x_{x;t} + 1); \tag{3.14}$$

$$S_J \quad = \frac{E_{C_0}}{2}(G_{x;x}(1 \quad 2J_{x;t}) \quad 2 \sum_{x^0 \neq x} G_{x;x^0}J_{x^0;t}): \tag{3.15}$$

Now, let us consider S_Q. For convenience, let us split Q into two parts where the first depends on the $q_{x;}$ -variables and the other on the $J_{x;}$ -variables. We denote the difference in Q between two states as Q. We then have that

$$\begin{aligned} S_Q = S_Q[Q + \quad Q] \quad S_Q[Q] = \sum \frac{E_C}{2}(Q^2 + 2Q \quad Q \ ); \\ Q \quad = Q^{(1)} + Q^{(2)}; \quad Q^{(1)} = \sum_j q_{j;} \ ; \quad Q^{(2)} = \quad {}^2 \sum_i J_{i;} \ (G_{i;L_x} \quad G_{i;1}): \end{aligned} \tag{3.16}$$

Now, the task is to compute $Q = Q^{(1)} + Q^{(2)}$. The latter part is easy and can be done just as before: $Q^{(2);} = Q^{(2);}[J_{x;t} \quad _{x;t}] \quad Q^{(2);}[J_{x;t}]$. This yields

$$\begin{aligned} Q^{(2);\ x} = 0; \\ Q^{(2);} \quad = \quad {}^2(G_{x;L_x} \quad G_{x;1}): \end{aligned} \tag{3.17}$$

Now, consider $Q^{(1)}$. The problem that arises is that we need to compute the difference in the $q_{x;}$ -values even when the worm is not closed. This is resolved by devising a way to use "imaginary link-currents" to close the worm. This allows us to find the $q_{x;}$ variables, even when the worm is not closed. There are many different schemes to close the worm, however some are more efficient than others. We will use the following scheme (see figure 3.2) which conveniently puts $Q^{(1);\ x} = 0$:

1. When the worm attempts to move in any direction, we must consider two scenarios; one where the move in accepted, and one where the move is rejected (green and red link-currents in figure 3.2, respectively). Consider first the scenario where the move is accepted.

2. The path is closed by first moving the worm in the x-direction to the starting x-coordinate x_0 and then by unwinding in the -direction until the worm has moved to $_0$.

3. Define a ground plaquette where $q_{x;} = 0$ outside the lattice. Then make a walk across the time-slice to assign values for $q_{x;}$ for all plaquettes on the time-slice. Each time an anticlockwise-oriented link-current $J_{x;}$ is crossed, _jH}09 0 the $q_{x;}$ with $jJ_{x;}\, j$. If a clockwise-oriented link-current is crossed, L0H}09 0 $q_{x;}$ with $jJ_{x;}\, j$.

4. Do step 2 and 3 again but this time do not accept the move. This is the reject scenario (red link-currents in figure 3.2).

5. Compute the difference $Q^{(1);} = \sum_j q_{j;}^{\text{acc}} \sum_j q_{j;}^{\text{rej}}$. Note that the "end" plaquettes should not be included in the sum.

A benefit with this scheme, besides the fact that $Q^{(1);\ x} = 0$, is that only the $q_{x;}$ -variables on one time-step needs to be computed. Combining this scheme with (3.16) and (3.17) we get that:

$$S_Q{}^x = 0; \tag{3.18}$$

$$S_Q = \frac{E_C}{2}(Q^2 + 2Q \quad Q\ ); \tag{3.19}$$

where

$$Q = \sum_j q_{j;}^{\text{acc}} \sum_j q_{j;}^{\text{rej}} \quad {}^2(G_{x;L_x} \quad G_{x;1}): \tag{3.20}$$

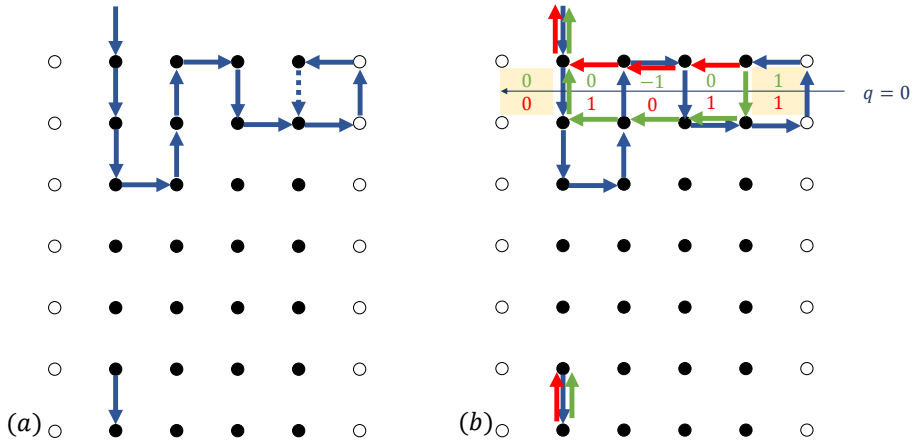

Figure 3.2: An illustration of the computation of the $q_{x;}$ -variables. (a) shows the worm proposing of doing the update $J_{4;5}$! $J_{4;5}$ 1. (b) shows the added "imaginary link-variables" used to close the worm; the green link-variables constitute the accept scenario and the red the reject scenario. The colored numbers are the values of $q_{x;5}$ on each plaquette for the two scenarios. The values on the end plaquettes should not be included. In this example, $\sum_j q^{\text{acc}}_{j;} = 0 \quad 1 + 0 = \quad 1$ and $\sum_j q^{\text{rej}}_{j;} = 1 + 0 + 1 = 2$.

g n®_jX §\O °n}h n«§ T}nh 9jL _j§n §\O `n Oq\ nj H\9_j

The acceptance rates for movement in and out from the Josephson chain is determined by (2.87) and (2.89). Adding a link at position $(x; t)$ where x 2 $fL_x; 0g$, in the x direction, gives a change $S^{\ x}_{L_x=0\text{J\_j}\S} = S_{L_x=0\text{J\_j}\S}[J^x_{x;t} \quad _{x;t}] \quad S_{L_x=0\text{J\_j}\S}[J^x_{x;t}]$, where L_x=0 stands for movement in the right and left transmission line, respectively. After some simplification one gets:

$$S^{\ x}_{L_x=0\text{J\_j}\S} = \frac{2\ R}{R_Q L} \sum_{s;s'=0}^{L\,X\,1} (J^x_{L_x=0}(s) \quad _{t;s})(J^x_{L_x=0}(s') \quad _{t;s'})$$

$$J^x_{L_x=0}(s)J^x_{L_x=0}(s') \quad B_{s;s'} \tag{3.21}$$

$$= \frac{2\ R}{R_Q L} \left[\sum_{s=0}^{L\,X\,1} J^x_{L_x=0}(s)B^{\prime}_{s;t} + \frac{B^{\prime}_{t;t}}{2} \right];$$

where we defined

$$B^{\prime}_{s;t} \quad B_{s;t} + B_{t;s} = \sum_{n=1}^{L\,X\,1} \frac{\cos \ !_n \quad (s \quad t)}{j \sin \frac{!_n}{2} j}: \tag{3.22}$$

g n®_jX §\0 °n}h _j §\0 §}9j h_ _nj e_j0

So far, we have considered movement in the Josephson chain, and when the worm enters or leaves the chain. What about movement in the time-direction in the transmission line i.e. when the head of the worm is at $x = 0$ or $x = L_x + 1$? This will change the value of the $q_{x;}$ -variables on that time-step. This means we will need to include a cost S_Q for this movement. However, we see that only $Q^{(1)}$ contributes.

A further complication of this is that, since the "end plaquettes" are not counted, then if the starting position x_0 1 or x_0 L_x, then $S_Q = 0$ is always true if $x = 0$ or $x = L_x + 1$, respectively. This will make the acceptance rate for movement in the transmission line be 1. In the simulations this will lead to a situation where the worm is very likely to move to the transmission line and "wind up" in the time-direction, and it will have very difficult to find its starting position again. For this reason, the worm is restricted to have a maximum extent in the time-direction, i.e. W L .

¨u¨ |0e0®9j§ q9}9h0§0} 9jL H\nn _jX Δ

As mentioned in chapter 2, the relevant parameters in our problem are the superconducting stiffness $K = \sqrt{E_J/E_C}$, the screening length $= \sqrt{C/C_0}$ and the dimensionless resistance R/R_Q. The inverse temperature $= L$ is naturally also important. However, many of the S:s described above contains a factor of E_C , which we want to be expressed in terms of K, and R/R_Q. If we choose appropriately this can be done. We have namely four time-scales in our problem, the first of which is the inverse plasma frequency $1/! = 1/\sqrt{E_J E_C}$. For smaller values of we should also consider the time scale $1/\sqrt{E_J E_{C_0}}$ which is the time scale for the phase fluctuations of a single island. Separately from these, we have time scale of the RC-circuit; $RC = \frac{R}{\sim}\frac{(2e)^2}{(2e)^2}C = \frac{2}{R_Q}\frac{R}{E_C}$. Naturally, we should also consider the time-scale RC_0.

When running a simulation, the smallest of these time-scales was chosen. To obtain converging simulation results, it was also needed to include a factor $f > 1$ in these time-scales, i.e. we have that:

$$\begin{aligned} &\frac{1}{f}\min\left(\frac{1}{\sqrt{E_J E_C}}; \frac{1}{\sqrt{E_J E_{C_0}}}; \frac{2}{R_Q}\frac{R}{E_C}; \frac{2}{R_Q}\frac{R}{E_{C_0}}\right) \\ &= \frac{1}{fE_C}\min\left(\frac{1}{K}; \frac{1}{K}; \frac{2}{R_Q}\frac{R}{}; \frac{2}{{}^2R_Q}\right)_{\max}: \end{aligned} \tag{3.23}$$

The working principle behind the choice of parameters is as follows:

1. Choose a temperature and express it in terms of E_C i.e. $= k/E_C$ where k is a chosen number. Choose interesting values of K, and R/R_Q.

2. Choose a value $f > 1$ and determine the maximum value of $E_{C\ \max}$ according to (3.23).

3. Compute L as $L = H0\_e(\ =\ _{\max})$. Then find the actual time-step as $E_C = E_C\ =L$.

4. Repeat step 2-3 for different values of f until the results converge.

The quantity sampled in the simulations is the effective inverse capacitance $C^{-1}_{k=0}$ discussed in section 2.7. Deep in the superconducting state $C^{-1}_{k=0}$ should approach 0, and deep in the insulating state $C^{-1}_{k=0}$ approaches L_x 1.

We now have all our building blocks needed to generate our Monte Carlo simulations. The next section gives an overview of the algorithm and a few comments on the code implementation of it.

¨uV m®0}®_0° nT §\0 9eXn}_§\h

1. Choose values for K, and $R=R_Q$. Choose a value k and write the inverse temperature as $= k=E_C$.

2. Choose a value of $f > 1$ and compute L and E_C according to the procedure described in section 3.3.

3. Start generating closed loops on the lattice. The first N_{equil} loops should be used to get the system into equilibrium and no data should be sampled after each loop. The loops are generated in the following way:

   3.1. Choose a random starting site $s_0 = (x_0;\ _0)$ where $x_0\ 2\ [0; L_x + 1]$ and $_0\ 2\ [0; L\ \ 1]$.

   3.2. Choose a direction $= x;$ out of the possible directions with uniform probability, with the condition that $jW\ j\ \ L$. The change acceptance rate A_{s_i} for adding a link in that direction is computed in the following way:

   ^T (== x)

   ^T ((x_i == 0 and == +x) or (x_i == L_x + 1 and == x))
   then $A_{s_i}{}^x = \min(1; 3=4e^{\ S^{\ x}_{L_x=0;\_j\S}})$ where $S^{\ x}_{L_x=0;\_j\S}$ is given by (3.21)

   0e 0 _T ((x_i == 1 and == x) or (x_i == L_x and == x))
   then $A_{s_i}{}^x = \min(1; 4=3e^{\ S^{\ x}_{L_x=0;\_j\S}})$ where $S^{\ x}_{L_x=0;\_j\S}$ is given by (3.21)

   0e 0
   then $A_{s_i}{}^x = \min(1; e^{\ S_J{}^x})$ where $S_J{}^x$ is given by (3.14)

   0 j L

Oe O _T (==)
_T (x 2 [1; L_x])
then A_{s_i} = min(1; e $^{(\ S_J\ +\ S_Q\ )}$) where S_J and S_Q is given by (3.15) and (3.19), respectively.
Oe O
then A_{s_i} = min(1; e ^{S_Q}) where S_Q is given by (3.19).
OjL
OjL

3.3. With probability A_{s_i}, move the head of worm from the site s_i to the new site s_{i+1}. With probability 1 A_{s_i}, go to 3.2.

3.4. Update the correct link-current $J^{j\ j}_{x;}$ and the Q = $\sum_x q_{x;}$ -variable.

3.5. Repeat step 3.2-3.4 until $s_i = s_0$ and $W = 0$.

4. Repeat steps 3.1-3.5 $N_b N_{prod}$ times where N_b stands for the number of blocks and N_{prod} for the number of generated loops in each block. This time sample the value of $Q = \sum Q$ after each generated loop.

5. Compute $C_{k=0}^{1}$ in each block separately and estimate the error using (3.12).

6. Repeat steps 2-5 for increasing values of f until the results converge.

¨uVuo 8 TO° Hnh h0j§ nj §\0 HnL0 _h qe0h0j§9§_nj

The implementation of the algorithm described above was done in C++. The code used to generate the results presented in chapter 4 can be found at \§§q I ¤¤X_§\«@uHnh¤}}0j@0}Xb¦[¤h9 §0}¬§\0 _ .

Let us first discuss the storage of the variables in the algorithm. For efficiency, $G_{i;i'}$ and $B^{l}_{s;}$ can computed before the generation of worms starts, and the values can be put in look-up tables. The $J^{x}_{x;}$ - and $J_{x;}$ -variables can comfortably be represented as integer arrays of size $(L_x + 1)$ L and $(L_x + 2)$ L , respectively. The Q -variables can be represented as an array of doubles of length L . The values of these arrays are updated after each accepted move of the worm, and they are kept after each closed loop.

In addition to this, we also have "worm variables" $J^{x;\mathrm{worm}}_{x;}$ and $J_{x;}^{;\mathrm{worm}}$ which are initialized at the creation of each new worm. These represent the worm that is currently being generated and are used to compute $Q^{(1)}$. It is also useful to have an integer variable W which records the distance between the head and the tail of the worm in the -direction.

In Monte Carlo simulations, the generation of (pseudo-)random numbers is a necessity. In our case, random numbers are used to choose directions for the worm to move and to determine the whether a move is to be accepted. There are many options for a random number generator. The generator should be fast, and the

generated numbers should ideally be uncorrelated and have an infinite period. In this thesis, we used the Mersenne Twister engine [34, 35].

The computation time to generate a closed loop is naturally strongly correlated to the system size L_x L . This limits which temperatures and which values of L_x, R/R_Q, , f and K that are possible to simulate. The largest system size used in this thesis is ca. 3800 (this is for $L_x = 40$, $= 400/E_C$ $R/R_Q = 100$, $f = 3$ and $= 0{:}1$). The most time-consuming single step in the algorithm is the computation of Q . Program profiling showed that this step took approximate 20 30% of the total CPU processing time.

G\9q§O} V

i « h O}_H9e }O «e§

In this chapter we present the results from the simulations. The chapter is divided into two sections. Section 4.1 is dedicated to investigating the dissipative phase transition predicted by Schmid and Bulgadaev (see section 2.3). We display results for both a single Josephson junction and for Josephson chains containing up to 19 junctions. Note that from section 2.3 corresponds to $R_Q=2R$ in our system, with an emphasis on the two, since there are two transmission lines in the system, each with a real impedance R.

In section 4.2 we investigate the phase transition in Josephson junction chains that occurs when $\sqrt{E_J=E_{C_0}}$ crosses the critical values predicted by Bradley and Doniach, and later by Choi et al. and Korshunov (see section 2.6).

In section 4.1 we study the effects of both long and short-ranged Coulomb interaction on the dissipative phase transition, by which we mean the values = 10 and = 0:1, respectively. Due to computational reasons, only the case of short-ranged Coulomb interactions is investigated in section 4.2. In each section, we also display the effect of increasing f, i.e. keeping the temperature constant but increasing L .

Vuo K_ _q9§_®O q\9 0 §}9j _§_nj

Vuouo dnjX]}9jXOL Gn«enh@ _j§0}9H§_nj

8 _jXeO `n Oq\ nj a«jH§_nj

Figure 4.1 displays $C_{k=0}^{-1}$ as a function of $2R/R_Q$ for a single Josephson junction.

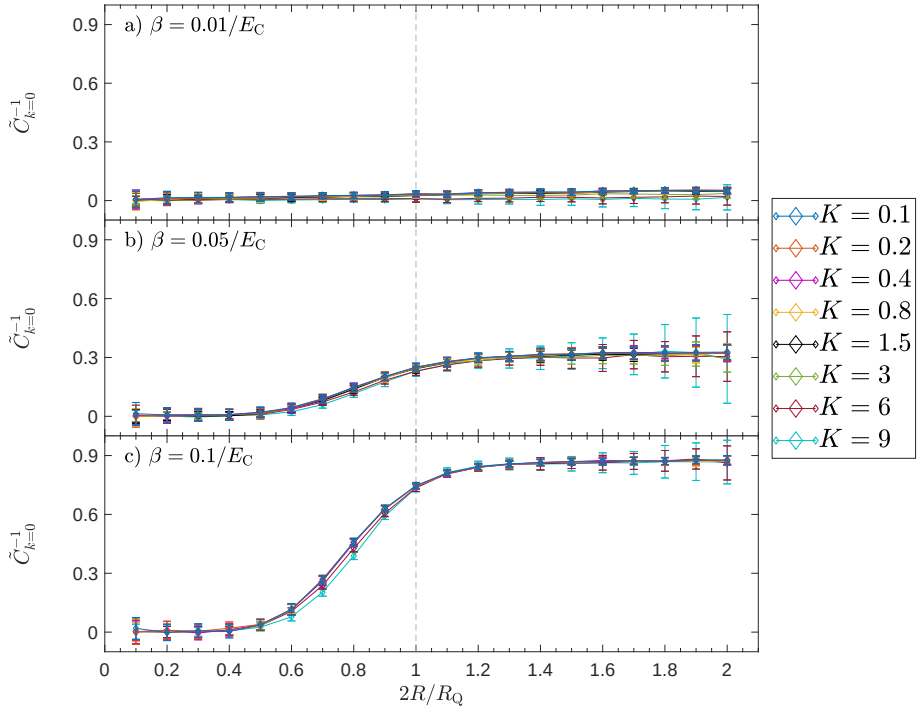

Figure 4.1: The effective inverse capacitance $C_{k=0}^{-1}$ as a function of $2R/R_Q$ for three temperatures and different values of $K = \sqrt{E_J/E_C}$. Other parameter values: $L_x = 2$, $= 10$, $N_{equil} = N_{prod} = 3$ 10^5, $N_b = 100$ and $f = 15$.

N¸OH§ nT _jH}O9 _jX f

Increasing the value of f, meaning keeping the temperature constant but increasing L , resulted in two effects (see figure 4.2):

1. The first effect appears only for relatively high temperatures (/ 0:1=E_C), for which L is relatively small, in particular for large values of $2R/R_Q$ and small values of K. This results in a large decrease of $C_{k=0}^{-1}$, as is illustrated in 4.2a. The sudden drops seen in the curve for $K = 0{:}4$; $f = 1$, corresponds to a

large relative decrease of the L . For example, the drop at $2R=R_Q$ = 0:7 0:8 corresponds to a decrease of L from 3 to 2, and that at $2R=R_Q$ = 1:5 1:6 corresponds to a decrease of L from 2 to 1. However, if L is large enough, i.e. if is small enough, this effect disappears.

2. The second effect from increasing the value of f is a sharper phase transition, see figure 4.2b. In contrast to the first effect, this does not seem to vanish for larger values of f.

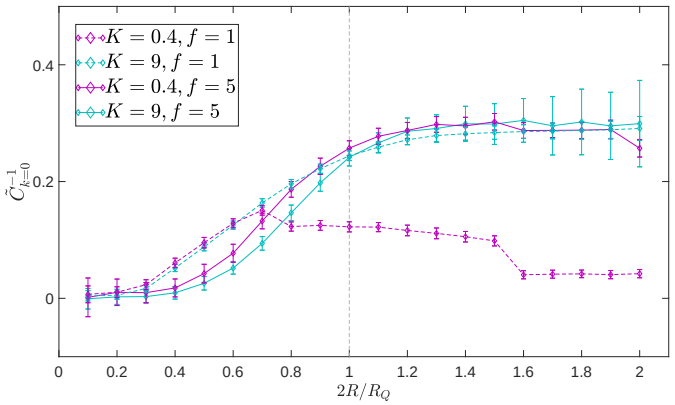

r9s

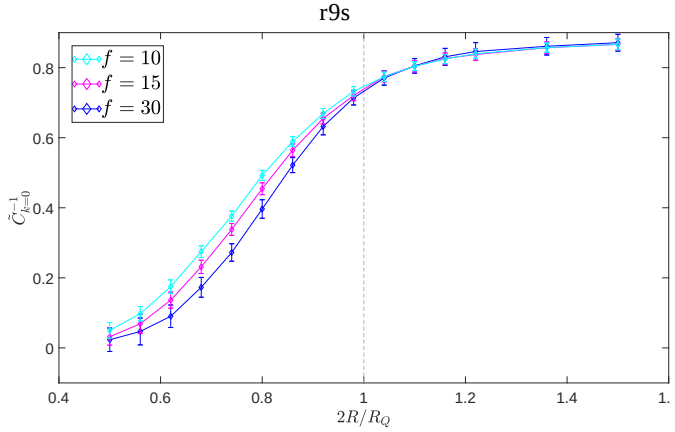

r@s

Figure 4.2: Plots used to illustrate the effect yielded from increasing f for = 10, i.e. the effect of increasing L . For details, see text. Common parameter values in both plots: L_x = 2, = 10, N_{equil} = N_{prod} = 3 10^5, N_b = 100. The inverse temperature in a) is = 0:05=E_C, and in b) we have E_C = 0:1= and K = $\sqrt{E_J=E_C}$ = 1 for all three curves.

8 `n Oq\ nj a«jH§_nj H\9_j

Figures 4.3 and 4.4 display the results for Josephson chains with 9 and 19 junctions, respectively. As can be seen, the qualitative behavior is much the same as for a single junction. Computational limitations restricted us in these cases to keeping f 2.

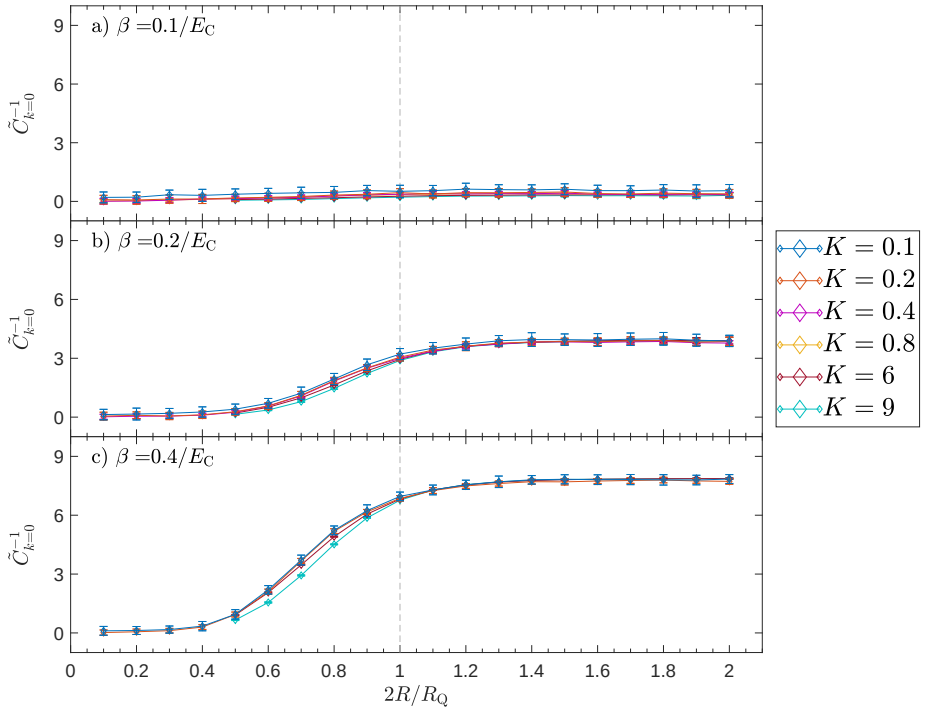

Figure 4.3: The effective inverse capacitance $\tilde{C}^{-1}_{k=0}$ as a function of $2R/R_Q$ for three temperatures and different values of $K = \sqrt{E_J/E_C}$. Other parameter values: $L_x = 10$, $= 10$, $N_{equil} = N_{prod} = 3 \quad 10^6$, $N_b = 100$. $f = 2$ in a) and b), and $f = 1$ in c).

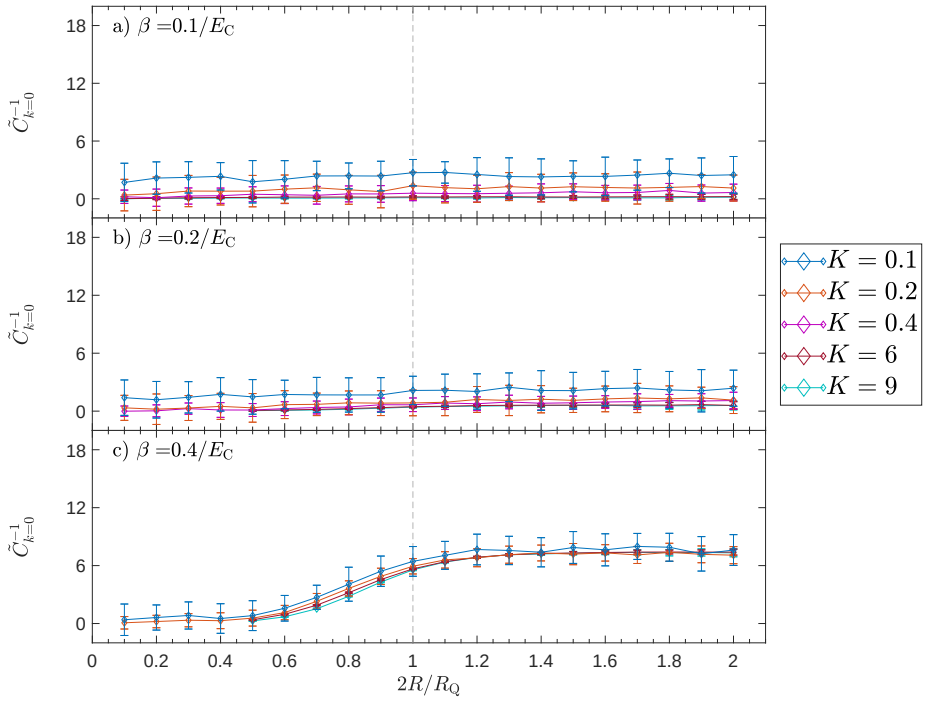

Figure 4.4: The effective inverse capacitance $\tilde{C}^{-1}_{k=0}$ as a function of $2R/R_Q$ for three temperatures and different values of $K = \frac{1}{\sqrt{E_J/E_C}}$. Other parameter values: $L_x = 20$, $= 10$, $N_{equil} = N_{prod} = 3 \quad 10^6$, $N_b = 100$. $f = 2$ in a) and b), and $f = 1$ in c).

Vuou© ~\n}§]}9jXOL Gn«en h@ _j§O}9H§_nj

8 _jXeO `n Oq\ nj a«jH§_nj

Figure 4.5 displays the results for a single Josephson junction with = 0:1. As can be seen, whether the junction is in a superconducting state or not seems to be independent on the dissipation strength but strongly dependent on K. Practically identical results were found for longer chains, which is why these results are not presented here. The effect of increasing f is discussed in section 4.2.

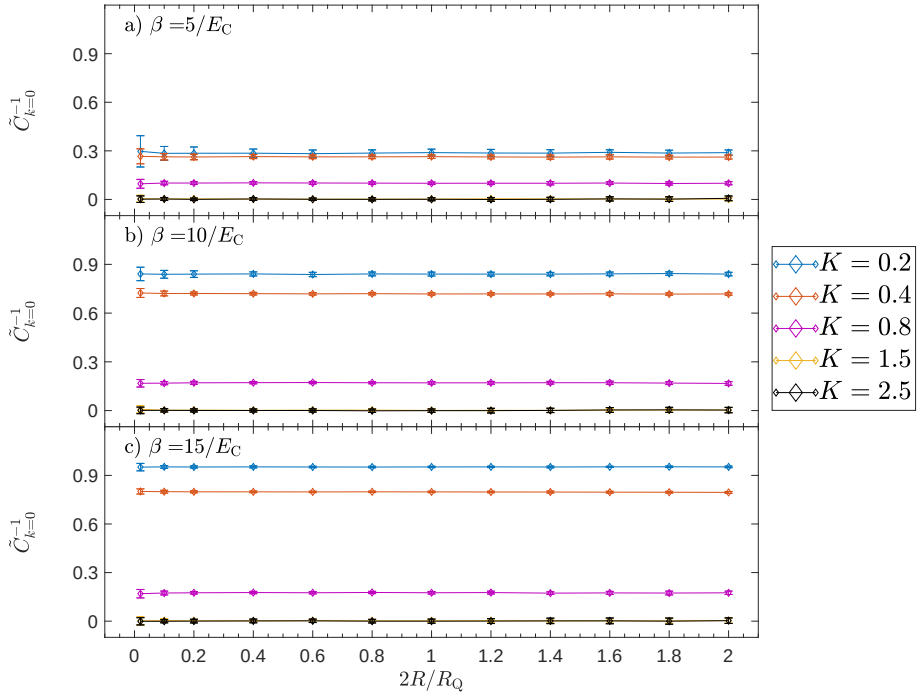

Figure 4.5: The effective inverse capacitance $\tilde{C}^{-1}_{k=0}$ as a function of $2R/R_Q$ for three temperatures and different values of $K = \sqrt{E_J/E_C}$. Other parameter values: $L_x = 2$, = 0:1, $N_{equil} = N_{prod} = 3$ 10^5, $N_b = 100$ and $f = 1$. Note that the curves for $K = 1{:}5$ and $K = 2{:}5$ overlap almost completely.

Vu© ?}9Le0´ŚKnj_9H\ q\9 0 §}9j _§_nj

In this section we investigate the phase transition that occurs for infinite Josephson junction chains when $\sqrt{E_J/E_{C_0}} = K/$ crosses a critical value, i.e. when K crosses K_c for a fixed . The transition becomes a crossover for finite chains at finite temperatures. Since we want to consider a system with free boundary conditions, i.e. no dissipation, we want a large value of R/R_Q. In plots 4.6 and 4.7 below we use $R/R_Q = 100$. Only the results for $= 0{:}1$ is presented below (see figure 4.6 below) since it was found that the computation time for the system sizes required to observe a phase transition for $= 10$ was too long. For $= 0{:}1$, we expect to find the critical value K_c in the interval $0{:}2/ < K_c < 0{:}079$ (see section 2.6).

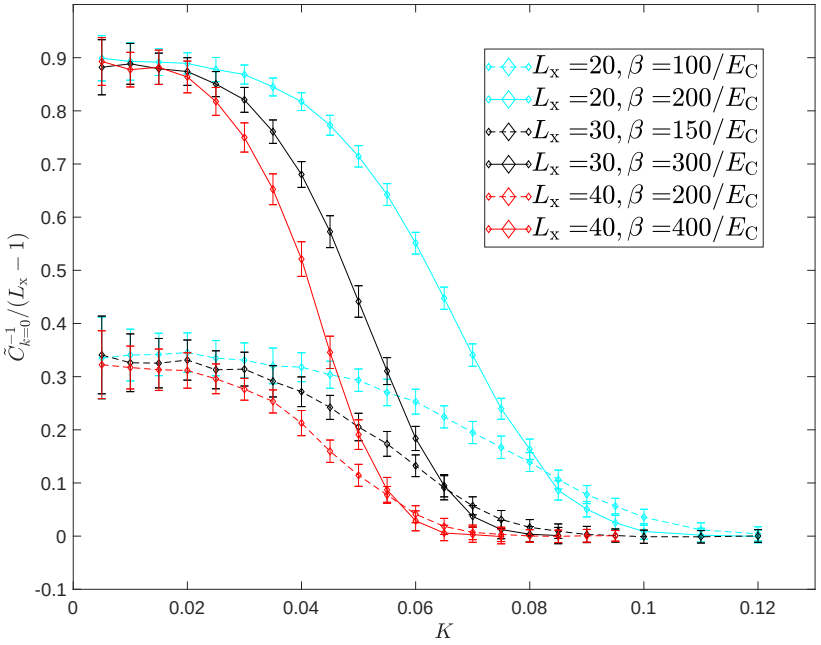

Figure 4.6: The effective inverse capacitance $C^{-1}_{k=0}$ as a function of $K = \sqrt{E_J/E_C}$ for three different chain lengths and parameter values $R/R_Q = 100$, $= 0{:}1$, $N_{equil} = N_{prod} = 10^6$, $N_b = 100$. $f = 5$ when $L_x = 20$ and $L_x = 30$, and $f = 3$ when $L_x = 40$.

N¸OH§ nT _jH}O9 _jX *f*

Figure 4.7 shows the effect of increasing f for = 0:1, i.e. keeping the temperature constant but increasing L . As can be seen, increasing f makes the curve smoother, until it converges for high enough values of L .

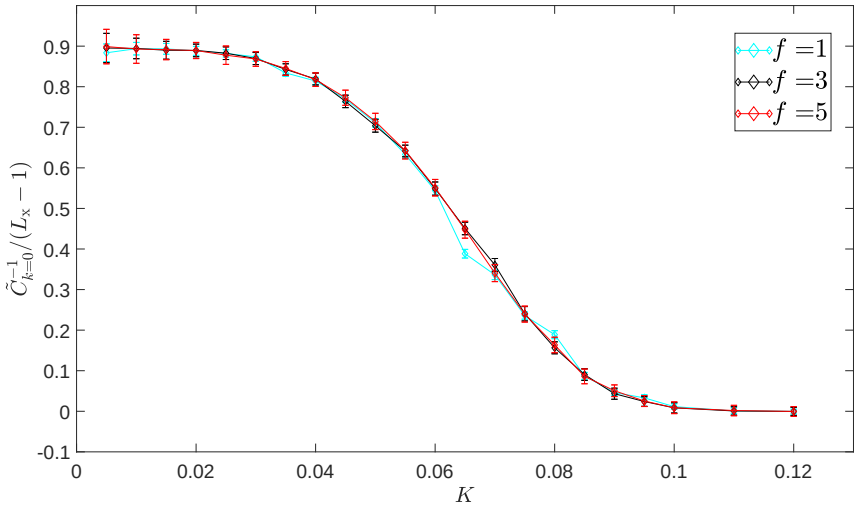

Figure 4.7: Plot used to illustrate the effect yielded from increasing f for = 0:1, i.e. the effect of increasing the L . As is shown, increasing f "smooth outs" the curve. The parameter values used are: L_x = 20, = 100=E_C, R=R_Q = 1, N_{equil} = N_{prod} = 10^6, N_b = 100.

G\9q§0} U

K_ H« _nj 9jL HnjHe« _nj

Let us first discuss the effect of the dissipative couplings on the system. For a single junction with long-ranged Coulomb interaction, the figures 4.1 and 4.2b seem to indeed indicate that a quantum phase transition occur at around $2R=R_{\mathrm{Q}}$ 1, however the exact position of the transition is difficult to determine. A finite size scaling technique or similar is likely needed to extract a critical value of the dissipation strength. The effect of lowering the temperature is that $C_{k=0}^{-1}$ increases for large values of $2R=R_{\mathrm{Q}}$, i.e. the insulating state becomes "more insulating", just as one would expect for a phase transition. For high temperatures, the insulating state does not appear at all.

There is a discrepancy between the Monte Carlo results found here and those found by Herrero and Zaikin [19], and the experimental results of Pentillä et al. [18]. As mentioned in previous chapters, the former found that that for finite temperatures, the transition becomes a crossover whose position is dependent on the value of K. This explanation is in agreement with the results of Pentillä et al. However, our results indicate that the transition point hardly depends on K at all. This discrepancy is yet to be explained.

Still keeping long-ranged Coulomb interaction and increasing the number of junctions to nine and 19 as is done in figures 4.3 and 4.4, respectively, the overall behavior of the system is the same as for a single junction, although the total inverse capacitance $C_{k=0}^{-1}$ is naturally larger. This agrees with the theory of section 2.6. To see a larger effect when varying K, a larger ratio $L_{\mathrm{x}}=$ is likely necessary.

For the case of short-ranged Coulomb interaction, the system seems to not depend at all on the strength of dissipative couplings, as is displayed in figure 4.5. An alternative explanation is that the phase transition has been moved to very small values of $2R=R_{\mathrm{Q}}$ which is not probed here. In any case, our simulations indicate that the dissipative phase transition is strongly dependent on . For intermediate values of , e.g. = 1, one is likely to find a behavior which lies in between those for = 10 and = 0:1. This dependence has, to our knowledge, has not been explicitly pointed out in other literature.

One can, however, for short-ranged Coulomb interaction, clearly see a dependence of the superconducting state on K (see figure 4.6). For an infinite chain at zero temperature, we expect a phase transition at $0{:}2 = < K < 0{:}079$ (see section 2.4). From figure 4.6 we see that the critical value of K seems to decrease as the length of the chain increases, and that the transition becomes sharper when the temperature is lowered. However, again without a finite size scaling technique, it is difficult to determine an exact transition point.

Let us also comment on the effect of decreasing the time-step , i.e. increasing f. As illustrated, decreasing the time-step for long-ranged Coulomb interaction had two major effects: it increased the value of $C_{k=0}^{-1}$ for small values of L , and it made the transition from a superconducting to an insulating state sharper. The former effect disappears for low enough temperatures, but the latter does seemingly not. For short-ranged Coulomb interaction, decreasing had an effect of smoothing the simulated transition. These effects indicate that choosing as we have done, together with $f = 1$, is only accurate for low temperatures. To study the behavior of the system for different temperatures, it might therefore be advantageous to choose a that is dependent on the temperature.

The effective inverse capacitance $C_{k=0}^{-1}$ also deserves some reflection. As the quantity used to detect the phase transitions, it is of key importance in this thesis. It might be experimentally measurable by embedding the system in a LC-circuit and relating it to the resonance frequency. Performing such experiments and comparing the results with ours may be of help to determine the accuracy of these simulations.

In conclusion, we have in this thesis used Monte Carlo simulations to investigate the superconductor-insulator phase transitions in Josephson junction chains coupled to a dissipative environment. Our results seem to confirm both the Schmid(-Bulgadaev) transition for a single junction, and the Bradley-Doniach transition for an infinite chain, however additional analysis is needed to extract exact critical values for the transitions. We have also demonstrated that the Schmid(-Bulgadaev) transition is clearly dependent on the charge screening length which, to our knowledge, is an effect that has not been explicitly pointed out in other literature. Nevertheless, some discrepancies were found between our results and those of other simulations and experiments. To explain these, further study is needed.

? _@e_nX}9q \ ´

[1] P. Mangin and R. Kahn, *~«q0}HnjL«H§_®_§´I 8j _j§}nL«H§_nj* (Springer International Publishing, Cham, 2017).

[2] M. Tinkham, *^j§}nL«H§_nj §n ~«q0}HnjL«H§_®_§´ r©jL NL_§_njs* (Dover Publications, 1996).

[3] R. Gross and A. Marx, Lecture notes of Prof. Gross and Dr. Marx to the Lecture on "Applied Superconductivity" (WS 2003/2004, WS 2004/2005, WS 2006/2007, WS 2007/2008, WS 2008/2009, WS 2009/2010, SS 2013, SS 2014, and SS 2015), 2015, URL: `\§§qI¤¤°°°u°h_u@9L°]h«OjH\OjuLO¤§O9H\_jX¤dOH§«}Ojn§O ¤`. Last visited on 2018/10/02.

[4] R. Fazio and H. van der Zant, *w«9j§«h q\9 0§}9j _§_nj 9jL ®n}§0² L´j9h_H _j «q0}HnjL«H§_jX j0§°n}c* , Physics Reports ¨UU, 235 (2001).

[5] R. M. Bradley and S. Doniach, *w«9j§«h ¼«H§«9§_nj _j H\9_j nT `n 0q\ nj a«jH§_nj* , Phys. Rev. B ¨·, 1138 (1984).

[6] S. E. Korshunov, *N¸OH§ nT L_ _q9§_nj nj §\0 en°]§0hq0}9§«}0 q}nq0}§_0 nT 9 §«jj0e]a«jH§_nj H\9_j*, Sov. Phys. JETP £P, 609 (1989).

[7] M. S. Choi *0§ 9eu*, *w«9j§«h q\9 0§}9j _§_nj _j `n 0q\ nj]a«jH§_nj H\9_j* , Phys. Rev. B U¢, R716 (1998).

[8] A. Caldeira and A. Leggett, *w«9j§«h §«jj0ee_jX _j 9 L_ _q9§_®0 ´ §0h*, Annals of Physics oVk, 374 (1983).

[9] A. Schmid, *K_¸« _nj 9jL dnH9e_¶9§_nj _j 9 K_ _q9§_®0 w«9j§«h ~´ §0h*, Phys. Rev. Lett. Uo, 1506 (1983).

[10] S. A. Bulgadaev, *p\9 0 L_9X}9h nT 9 L_ _q9§_®0 x«9j§«h ´ §0h*, Soviet Journal of Experimental and Theoretical Physics Letters ¨k, 315 (1984).

[11] J. F. Annett, *~«q0}HnjL«H§_®_§´J «q0}¼«_L J 9jL HnjL0j 9§0* (Oxford University Press, New York, 2004).

[12] C. Timm, Lecture notes: Theory of Superconductivity, 2016, URL: \§§q I¤¤ °°°uq\´ _cu§«]L}0 L0juL0¤<§_hh¤q0} nj9e¤§09H_jX¤§\ «q¬°oo¤. Last visited on 2018/10/02.

[13] S. M. Girvin, Circuit qed: superconducting qubits coupled to microwave photons, Quantum Machines: Measurement and Control of Engineered Quantum Systems, Oxford University Press, 2014.

[14] A. Ergül 0§ 9eu, dnH9e_¶_jX x«9j§«h q\9 0 e_q _j nj0]L_h0j _nj9e `n 0q\ nj a«jH§_nj H\9_j , New Journal of Physics oU, 095014 (2013).

[15] O. V. Astafiev 0§ 9eu, Gn\0}0j§x«9j§«h q\9 0 e_q, Nature VPV, 355 EP (2012).

[16] B. I. Halperin, G. Refael and E. Demler, |0 _ §9jH0 _j ~«q0}HnjL«H§n} , ©V (2010).

[17] K. Arutyunov, D. Golubev and A. Zaikin, ~«q0}HnjL«H§_®_§´ _j nj0L_h0j _nj, Physics Reports V£V, 1 (2008).

[18] J. S. Penttilä 0§ 9eu, ō~«q0}HnjL«H§n}]^j «e9§n} ¦}9j _§_njȲ_j 9 ~_jXe0 `n 0q\] nj `«jH§_nj, Phys. Rev. Lett. P©, 1004 (1999).

[19] C. P. Herrero and A. D. Zaikin, ~«q0}HnjL«H§n}]_j «e9§n} x«9j§«h q\9 0 §}9j _§_nj _j 9 _jXe0 `n 0q\ nj a«jH§_nj, Phys. Rev. B £U, 104516 (2002).

[20] P. Werner and M. Troyer, N¹H_0j§~_h«e9§_nj nT |0 _ §_®0e´~\«j§0L `n 0q\ nj `«jH§_nj , Phys. Rev. Lett. kU, 060201 (2005).

[21] M. Wallin 0§ 9eu, ~«q0}HnjL«H§n}]_j «e9§n} §}9j _§_nj _j §°n]L_h0j _nj9e L_}§´ @n nj ´ §0h , Phys. Rev. B Vk, 12115 (1994).

[22] J. E. Mooij 0§ 9eu, ~«q0}HnjL«H§n}Ś_j «e9§n} §}9j _§_nj _j j9jn°_}0 9jL j9jn°_}0 9}}9´ , New Journal of Physics o¢, 033006 (2015).

[23] J. Lidmar, Notes on Quantum phase slips in Josephson junction arrays (unpublished), 2016.

[24] A. Andersson and J. Lidmar, gnL0e_jX 9jL _h«e9§_nj nT x«9j§«h q\9 0 e_q _j «e§}9§_j «q0}HnjL«H§_jX °_}0 , Phys. Rev. B ko, 134504 (2015).

[25] M. J. Morgan, d9X}9jX_9j Tn}h«e9§_nj nT 9 §}9j h_ _nj e_j0, American Journal of Physics U£, 639 (1988).

[26] S. Chakravarty and A. Schmid, `n 0q\ nj a«jH§_nj Hn«qe0L §n 9j nq0j §}9j] h_ _nj e_j0I 8j 9qqe_H9§_nj §n §\0 §\0n}´ nT h9H}n Hnq_H x«9j§«h §«jj0e_jX, Phys. Rev. B ¨¨, 2000 (1986).

[27] I. Cacciari, P. Moretti and A. Ranfagni, K_ _q9§_nj 9jL §}9®0} 9e §_h0 _j `n 0q\ nj a«jH§_nj , Phys. Rev. B Po, 172506 (2010).

[28] H. P. Büchler, V. B. Geshkenbein and G. Blatter, w«9j§«h Se«H§«9§_nj _j ¦_j ~«q0}HnjL«H§_jX ¯_}0 nT S_j_§0 d0jX§\, Phys. Rev. Lett. k©, 067007 (2004).

[29] F. Altomare and A. M. Chang, mj0]K_h0j _nj9e ~«q0}HnjL«H§_®_§´ _j i9jn°_}0 (Wiley-VCH, 2013).

[30] M. E. J. Newman and G. T. Barkema, gnj§0 G9}en h0§\nL _j §9§_ §_H9e q\´ _H (Clarendon Press, Oxford, 1999).

[31] H. Gould, J. Tobochnik and C. Wolfgang, 8j ^j§}nL«H§_nj §n Gnhq«§0} ~_h] «e9§_nj g0§\nL I 8qqe_H9§_nj §n p\´ _H9e ~´ §0h r¨}L NL_§_njs (Addison-Wesley Longman Publishing Co., Inc., Boston, MA, USA, 2005).

[32] M. Plischke, Nx«_e_@}_«h §9§_ §_H9e q\´ _H , 3. ed.. ed. (World Scientific, Singapore, 2006).

[33] M. Kastner, gnj§0 G9}en h0§\nL _j §9§_ §_H9e q\´ _H I g9§\0h9§_H9e Tn«j] L9§_nj 9jL §}9§0X_0 , Communications in Nonlinear Science and Numerical Simulation oU, 1589 (2010).

[34] Mersenne twister 19937 generator, \§§qI¤¤°°°uHqe« qe« uHnh¤}OTO}OjHO¤ }9jLnh¤h§okk¨¢¤. Last visited on 2018/10/09.

[35] M. Matsumoto and T. Nishimura, g0} 0jj0 ¦°_ §0}I 8 £©¨]L_h0j _nj9ee´ Nx«_L_ §}_@«§0L ª j_Tn}h p 0«Ln]}9jLnh i«h@0} W0j0}9§n}, ACM Trans. Model. Comput. Simul. P, 3 (1998).

8 qq0jL_² 8

G9eH«e9§_n j nT $G_{i,i'}$

In this appendix we calculate the inverse of the capacitance matrix C given by (2.24). Since C is real and symmetric, it can be expressed as a sum of its normalized eigenvectors $'_n$ and eigenvalues $"_n$. Similarly, its inverse can be written as

$$C^{-1}_{i;i'} = \sum_n \frac{'_{n;i}\,'_{n;i'}}{"_n}: \tag{A.1}$$

From the eigenvalue equation $\mathbf{C}\,'_n = "_n\,'_n$ and (2.24), we get the three equations:

$$(C_0 + 2C)\,'_{n;x} \quad C\,'_{n;x+1} \quad C\,'_{n;x\ 1} = "_n\,'_{n;x}; \qquad 1 < x < L_x, \tag{A.2}$$

$$(C_0 + C)\,'_{n;1} \quad C\,'_{n;2} = "_n\,'_{n;1}; \qquad x = 1, \tag{A.3}$$

$$(C_0 + C)\,'_{n;L_x} \quad C\,'_{n;L_x\ 1} = "_n\,'_{n;L_x}; \qquad x = L_x. \tag{A.4}$$

We will make the ansatz $'_{n;x} = A_n \cos(!_n(x \quad 1) + \ )$. Thus, we have four unknowns: A_n, $!_n$, and $"_n$, and we have 4 equations: (A.2)-(A.4) and the normalization condition $1 = \sum_x '^2_{n;x}$. Inserting the ansatz into equation (A.2) yields

$$\cos(!_n(x \quad 1) + \ )(C_0 + 2C \quad "_n) = C[\cos(!_n x + \ ) + \cos(!_n(x \quad 2) + \ )]: \tag{A.5}$$

From this we can find

$$"_n = C_0 + 2C(1 \quad \cos(!_n) = C_0 + CH_n^2; \tag{A.6}$$

where $H_n \quad 2 \quad 2\cos(!_n) = 4\sin^2(\frac{!_n}{2})$.

Now, inserting the ansatz and the value for $''_n$ given by (A.6) into (A.3) yields (after dividing both sides by $'_{n;1}$ and some simplifications):

$$\frac{\cos(!_n + \quad)}{\cos(\quad)} = 2\cos(!_n) \quad 1: \tag{A.7}$$

Using the cosine addition formula $\cos(!_n + \quad) = \cos(!_n)\cos(\quad) \quad \sin(!_n)\sin(\quad)$, (A.7) can after some simplifications be written as

$$\cos(\quad) = \cos(!_n)\cos(\quad) + \cos(!_n)\sin(\quad) = \cos(!_n \qquad); \tag{A.8}$$

from which we find

$$= \frac{!_n}{2}: \tag{A.9}$$

Now, inserting $''_n$ into (A.4) yields after some simplifications:

$$'_{n;L_x} \quad '_{n;L_x \ 1} = H_n^2 \, '_{n;L_x}: \tag{A.10}$$

Inserting the ansatz and given by (A.9), this expression simplifies to

$$\frac{\cos(!_n(L_x^0 \quad \frac{1}{2}))}{\cos(!_n(L_x^0 + \frac{1}{2}))} = 2\cos(!_n) \quad 1 = 1 \quad 4\sin^2 \frac{!_n}{2} \ ; \tag{A.11}$$

where we have introduced $L_x^0 \quad L_x \quad 1$. Again, using the cosine addition formula on the numerator and denominator, this expression simplifies to

$$\begin{aligned} &\sin(!_n L_x^0)\sin\frac{!_n}{2} = \\ &= 2\sin^2\frac{!_n}{2}\cos(!_n L_x^0)\cos\frac{!_n}{2} \quad \sin(!_n L_x^0)\sin\frac{!_n}{2} \\ &) \ 1 = 2\sin\frac{!_n}{2}\cos\frac{!_n}{2}\frac{1}{\tan !_n L_x^0} \quad \sin\frac{!_n}{2} \ : \end{aligned} \tag{A.12}$$

Using that $1 \quad 2\sin^2\frac{!_n}{2} = \cos !_n$, (A.12) can after some reordering be formulated as

$$0 = \sin(!_n L_x^0)\cos(!_n) + \sin(!_n)\cos(!_n L_x^0) = \sin(!_n(L_x^0 + 1)); \tag{A.13}$$

from which we find

$$!_n = \frac{n}{L_x^0 + 1} = \frac{n}{L_x}: \tag{A.14}$$

Now, the remaining unknown variable is A_n. Inserting $!_n$ and into the ansatz we get that

$$'_{n;x} = A_n \cos \quad !_n \ x + \frac{1}{2} \quad = A_n \cos \frac{n \ (x + \frac{1}{2})}{L_x} \ ; \tag{A.15}$$

where $n = 0; 1; 2; \ldots; L_x - 1$. The normalization conditions then yield

$$1 = \sum_{x=1}^{L_x} \phi_{n;x}^2 = A_n^2 \sum_{x=1}^{L_x} \cos^2\left(\omega_n(x + \tfrac{1}{2})\right) = \frac{A_n^2}{2} \sum_{x=1}^{L_x} (1 + \cos(\omega_n(2x + 1))): \quad \text{(A.16)}$$

We have that $\sum_{x=1}^{L_x} \cos(\omega_n(2x + 1)) = L_x$ if $n = 0$, and otherwise it is 0. Thus, we can write

$$1 = \frac{A_n^2}{2}(L_x + L_x \delta_{n;0}) \;\Rightarrow\; A_n = \sqrt{\frac{2}{L_x(1 + \delta_{n;0})}}: \quad \text{(A.17)}$$

Finally, using (A.1), the inverse of $\mathbf{C}$ can be expressed as

$$\begin{aligned} C^{-1}_{i;i'} &= \sum_{n=0}^{L_x-1} \frac{\phi_{n;i}\,\phi_{n;i'}}{\lambda_n} = \sum_{n=0}^{L_x-1} \frac{1}{C_0 + CH_n^2} A_n^2 \cos\left(\omega_n(i + \tfrac{1}{2})\right) \cos\left(\omega_n(i' + \tfrac{1}{2})\right) \\ &= \frac{1}{C_0}\,\frac{1}{L_x} + \frac{2}{L_x} \sum_{n=1}^{L_x-1} \frac{1}{1 + \alpha^2 H_n^2} \cos\left(\omega_n(i + \tfrac{1}{2})\right) \cos\left(\omega_n(i' + \tfrac{1}{2})\right) \\ &= \frac{1}{C_0}\,\frac{1}{L_x} + \frac{1}{L_x} \sum_{n=1}^{L_x-1} \frac{1}{1 + \alpha^2 H_n^2}\, \cos\left(\omega_n(i - i')\right) + \cos\left(\omega_n(i + i' + 1)\right) \\ &= \frac{1}{C_0}\,\frac{1}{L_x} + G^0(i - i') + G^0(i + i' + 1) - \frac{1}{C_0} G_{i;i'}; \end{aligned} \quad \text{(A.18)}$$

where

$$G^0(x) - \frac{1}{L_x} \sum_{n=1}^{L_x-1} \frac{1}{1 + \alpha^2 H_n^2} \cos(\omega_n x) = \frac{1}{L_x} \sum_{n=1}^{L_x-1} \frac{\cos\frac{n}{L_x}x}{1 + 4\alpha^2 \sin^2\frac{n}{2L_x}}: \quad \text{(A.19)}$$